Disponible en ligne sur www.sciencedirect.com
ScienceDirect
Revue de micropaléontologie 50 (2007) 27–57
Revue de micropaléontologie
http://france.elsevier.com/direct/REVMIC/

Original article

Early to Middle Devonian miospores from northern Saudi Arabia

Miospores du Dévonien Inférieur à Moyen au nord de l'Arabie Saoudite

Pierre Breuer[a,*], Abdullah Al-Ghazi[b,c], Mansour Al-Ruwaili[b], Kenneth T. Higgs[d], Philippe Steemans[a], Charles H. Wellman[c]

[a] *Laboratoire de paléobotanique, paléopalynologie et micropaléontologie, université de Liège, allée du 6-août, B18, Sart-Tilman, 4000 Liège, Belgium*
[b] *Saudi Aramco, P.O. Box 10781, 31311 Dhahran, Saudi Arabia*
[c] *Department of Animal and Plant Science, University of Sheffield, Alfred Denny Building, Western Bank, Sheffield S10 2 TN, United Kingdom*
[d] *Department of Geology, University College Cork, Cork, Ireland*

Abstract

Well-preserved palynomorph assemblages are recovered from the Devonian Jauf and Jubah formations in five shallow boreholes in the northern part of Saudi Arabia. These fully cored boreholes overlap stratigraphically to form a 1640 ft composite sequence. Miospores dominate the palynological assemblages of most samples. The assemblages are mainly composed of trilete spores but also contain cryptospores and monolete spores. One new genus, sixteen new species and two new varieties of miospores are described from the studied assemblages: *Artemopyra inconspicua* nov. sp., *Artemopyra recticosta* nov. sp., *Camarozonotriletes filatoffii* nov. sp., *Camarozonotriletes rugulosus* nov. sp., *Cymbohilates baqaensis* nov. sp., *Cymbohilates comptulus* nov. sp., *Cymbohilates heteroverrucosus* nov. sp., *Cymbosporites asymmetricus* nov. sp., *Dibolisporites pilatus* nov. sp., *Dictyotriletes biornatus* nov. sp., *Gneudnaspora divellomedia* (Chibrikova) Balme, 1988 var. *divellomedia*, *Gneudnaspora divellomedia* (Chibrikova) Balme, 1988 var. *minor* nov. var., *Latosporites ovalis* nov. sp., *Scylaspora costulosa* nov. sp., *Squamispora arabica* nov. gen. and sp., *Stellatispora multicostata* nov. sp., *Zonotriletes armillatus* nov. sp. and *Zonotriletes simplicissimus* nov. sp. Their stratigraphic distribution is compared to the well-established Devonian West European zonation of Streel et al. (1987) (Streel, M., Higgs, K.T., Loboziak, S., Riegel, W., Steemans, P., 1987. Spore stratigraphy and correlation with faunas and floras in the type marine Devonian of the Ardenne-Rhenish region. Review of Palaeobotany and Palynology 50, 211–219). A late Pragian-Givetian age is suggested for this sequence. No characteristic Eifelian taxa are recorded, but this could be explained by a gap in palyniferous samples.

Résumé

Des assemblages palynologiques bien conservés ont été retrouvés dans les formations de Jauf et de Jubah traversées par cinq forages situés dans le nord de l'Arabie Saoudite. Ces forages se chevauchent stratigraphiquement et forment une séquence composite de 1640 pieds. Les miospores dominent les assemblages palynologiques de la plupart des échantillons. Les assemblages sont principalement composés de spores trilètes mais ils contiennent également des cryptospores et des spores monolètes. Un nouveau genre, seize nouvelles espèces, deux nouvelles variétés de miospores sont décrits à partir des assemblages étudiés : *Artemopyra inconspicua* nov. sp., *Artemopyra recticosta* nov. sp., *Camarozonotriletes filatoffii* nov. sp., *Camarozonotriletes rugulosus* nov. sp., *Cymbohilates baqaensis* nov. sp., *Cymbohilates comptulus* nov. sp., *Cymbohilates heteroverrucosus* nov. sp., *Cymbosporites asymmetricus* nov. sp., *Dibolisporites pilatus* nov. sp., *Dictyotriletes biornatus* nov. sp., *Gneudnaspora divellomedia* (Chibrikova) Balme, 1988 var. *divellomedia*, *Gneudnaspora divellomedia* (Chibrikova) Balme, 1988 var. *minor* nov. var., *Latosporites ovalis* nov. sp., *Scylaspora costulosa* nov. sp., *Squamispora arabica* nov. gen. et sp., *Stellatispora multicostata* nov. sp., *Zonotriletes armillatus* nov. sp. et *Zonotriletes simplicissimus* nov. sp. Leur distribution stratigraphique est comparée à la zonation dévonienne de Streel et al. (1987) (Streel, M., Higgs, K.T., Loboziak, S., Riegel, W., Steemans, P., 1987. Spore stratigraphy and correlation with faunas and floras in the type marine Devonian of the Ardenne-Rhenish region. Review of Palaeobotany and Palynology 50, 211–219) établie sur le continent Européen. Un âge Praguien supérieur à Givetien est suggéré pour cette séquence. Aucun taxon caractéristique de l'Eifelien n'a été trouvé, ceci pourrait être expliqué par une lacune d'échantillons productifs.

Keywords: Devonian; Miospores; Biostratigraphy; Saudi Arabia

Mots clés : Dévonien ; Miospores ; Biostratigraphie ; Arabie Saoudite

* Corresponding author.
E-mail address: piet79@yahoo.fr (P. Breuer).

0035-1598/$ – see front matter © 2007 Elsevier Masson SAS. All rights reserved.
doi:10.1016/j.revmic.2007.01.009

1. Introduction

During the Devonian, Arabia formed part of the northern passive margin of Gondwana, and lay just in southern tropical latitudes (Beydoun, 1991). Much of Arabia was subaerially exposed, with shallow seas extending over the remaining area. Substantial Devonian deposits accumulated, essentially as broad transgressive-regressive cycles: a retrogradational cycle (fining-upward) encompassing the Tawil and Jauf formations, and a progradational cycle (coarsening-upward) through much of the Jubah Formation (Sharland et al., 2001). Most of these deposits occur in subsurface, although limited surface outcrops abut against the Precambrian Arabian Shield in the northwest and southwest of Saudi Arabia. Palynology (particularly dispersed plant spores) is the primary tool used in biostratigraphical dating and correlation of the Devonian deposits of Arabia supplementing marine faunas that are confined to the Jauf Formation (Boucot, 1984; Boucot et al., 1989). To date, however, only relatively few publications document the taxonomy and distribution of dispersed spores in the Devonian of Arabia (Hemer and Nygreen, 1967; Loboziak and Streel, 1995; Steemans, 1995; Al-Hajri et al., 1999; Loboziak, 2000). Recently, Saudi Aramco drilled a number of fully cored shallow boreholes in northern Saudi Arabia with the intention of shedding light on the nature of the Devonian deposits of this area. This paper reports on a palynological investigation of these boreholes. The aims of this paper are twofold:

- to describe in detail the taxonomy of Early and Middle Devonian spores from these boreholes;
- to document the stratigraphical distribution of the spores in order elucidate the age of the deposits, and possibly to facilitate establishing a local biostratigraphy.

2. Geological setting

The Devonian strata of Saudi Arabia occur within a conformable package of Late Silurian-earliest Carboniferous deposits, that are subdivided into the Tawil, Jauf and Jubah formations (Steineke et al., 1958; Powers et al., 1966; Powers, 1968; Meissner et al., 1988). A regional disconformity separates this package from older (middle Silurian: Wenlock) deposits of the underlying Qalibah Formation. Regional unconformities also separate this package from younger strata above: either the pre-Unayzah Unconformity (from the Permo-Carboniferous Unayzah Formation) or the pre-Khuff Unconformity (from the Upper Permian Khuff Formation). Current understanding of the ages of these deposits suggests that the oldest deposits of the Tawil Formation, occurring directly above the disconformity, are of Late Silurian (Ludlow-Pridoli) age, and the youngest parts are of the formation of Early Devonian (Pragian) age (Stump et al., 1995; Al-Hajri and Paris, 1998). The Jauf and Jubah formations are usually Emsian to Frasnian in age, although it has recently been discovered that in places the Jubah Formation deposits extend up into the latest Famennian to earliest Tournaisian (Al-Hajri et al., 1999; Clayton et al., 2000).

Lithologies are dominated by siliciclastics (Tawil Formation), mixed siliciclastics and carbonates (Jauf Formation) and a return to siliciclastics (Jubah Formation). The alternating siliciclastics and carbonates of the Jauf Formation have been used to subdivide this formation into five members: the Sha'iba (oldest), Qasr, Subbat, Hammamiyat and Murayr (youngest) members. The deposits of the Late Silurian-earliest Carboniferous package are generally continental to nearshore shallow marine. There are regional-scale facies changes. For example, the Jauf Formation changes from marine in northwestern Saudi Arabia to marginal marine/continental in central and southern regions (Al-Hajri et al., 1999; Al-Hajri and Owens, 2000).

Dispersed spores are the chief biostratigraphical tool utilized to date and correlate the deposits of the Tawil, Jauf and Jubah formations (Al-Hajri et al., 1999). It should be noted, however, that the occurrence of rich spore assemblages is sporadic. In many of the extensive sandstone and limestone sequences, rich spore assemblages are only recovered from thin siltstone/shale intercalations. Furthermore, as one moves east, burial depths of the Devonian deposits increase, and high thermal maturation levels negatively affect preservation of palynomorphs. Additional biostratigraphical evidence is provided by other fossil groups collected at the surface exposures (e.g., Boucot et al., 1989; Forey et al., 1992). For example, trilobites and conodonts indicate that the uppermost Sha'iba and Qasr members (lower Jauf Formation) are Pragian-early Emsian in age and brachiopods suggest that the Hammamiyat Member (upper Jauf Formation) is late Emsian in age.

3. Previous Devonian miospore studies in Saudi Arabia

Hemer and Nygreen (1967) were the first to report on spore assemblages from the Devonian of Saudi Arabia. These were from core and cuttings samples of a 1341 ft Devonian sequence in borehole S-462 in northern Saudi Arabia. They assumed that this interval represented a non-marine extension of the Jauf Formation that outcropped some 70 km away (but now considered as part of the Jubah Formation, see below). Based on spore assemblages they subdivided the strata into four zones: Zone I (1465–1670 ft, Upper Devonian assemblage); Zone II (1670–1940 ft, Upper Devonian); Zone III (1940–2300 ft, Middle Devonian); Zone IV (2700–2750 ft, probably Givetian, lower diversity assemblage in sandy facies).

Loboziak and Streel (1995) examined Devonian cuttings from borehole TRBH-1 also in northern Saudi Arabia, with additional data from boreholes DMMM-45 and SDGM-211 from eastern Saudi Arabia. Based on taxa common to the Euramerican region, they applied the Devonian spore zonation scheme developed in the Ardenne-Rhenish region by Streel et al. (1987). In all three wells, they assigned the spore assemblages from the uppermost Tawil and lower Jauf formations to the AB-FD Oppel Zone range (Emsian age). Higher in the sequence, in the Subbat Member of the Jauf Formation in boreholes TRBH-1 and DMMM-45, they recognized the FD (Min) and AP Oppel Zones (late Emsian age). Few characteristic spore taxa occurred above this latter zone in the Jubah Formation and Loboziak and Streel (1995) considered these strata to belong to an undifferentiated

AP-AD Oppel Zone range (latest Emsian to early Givetian). Stratigraphically above this, in borehole TRBH-1, occur assemblages they assigned to the AD (Lem) and TA Oppel Zones (Givetian).

Steemans (1995) published reports of Devonian spore assemblages from cuttings in boreholes DMMM-45 and UDYN-1. In DMMM-45, the miospores were recovered from the lower part of the Tawil Formation and assigned to the MN, BZ and PoW (W and Pa) Oppel Zones (Lochkovian to Pragian). Those recovered from the Jauf Formation were assigned to the AB Oppel Zone (Emsian). In UDYN-1, Steemans (1995) reported Lochkovian spore assemblages from the Tawil Formation (MN-R Interval Zone) and Givetian-Frasnian spore assemblages from the upper Tawil to lower Jauf formations.

Al-Hajri et al. (1999) provided a detailed description of the 'operational palynological zonation' developed by the oil industry for the Devonian strata of Saudi Arabia. Because it was developed by oil industry geologists working largely with borehole cuttings, this zonation is based primarily on first down-hole occurrence of taxa (i.e., extinctions), although it also considers first common down-hole occurrences/co-occurrences, and acme zones. The scheme consists of six zones and four subzones, from top to base: D0, D1, D2, D3A, D3B, D3/D4, D4A, D4B. These were age-calibrated based on comparisons with the established spore zonation schemes of Richardson and McGregor (1986) and Streel et al. (1987), that were both established in the Euramerican 'Old Red Sandstone' continent and the Ardenne-Rhenish region, respectively.

From the same sequence/borehole studied by Hemer and Nygreen (1967) (see above), Loboziak (2000) described spore assemblages from Jubah Formation cuttings of borehole S-462 from northern Saudi Arabia over the interval 1465–2806 ft. The oldest assemblages were interpreted to be of late early Eifelian age and the youngest of late early Frasnian age, again based on comparisons with the spore biostratigraphy scheme developed by Streel et al. (1987).

Clayton et al. (2000) described latest Devonian-earliest Carboniferous spore assemblages from the uppermost Jubah Formation in wells of eastern Saudi Arabia. In HRML-51, Strunian assemblages characterized by *Retispora lepidophyta* were recovered (D0 Palynozone of Al-Hajri et al., 1999). Latest Famennian and earliest Tournaisian assemblages in ABSF-29 were referred to the '*Verruciretusispora famenensis* Assemblage' and the '*Indotriradites explanatus* Assemblage', respectively. This work clearly demonstrates that in places the Jubah Formation extends into the Carboniferous.

4. Materials and methods

This study concerns cored boreholes drilled as part of the Saudi Aramco shallow core investigation of the Devonian deposits of northwestern Saudi Arabia. The studied boreholes are located in two distinct areas separated by ca. 350 km (Fig. 1). Two boreholes (BAQA-1 and BAQA-2) are near Baq'a in the Widyan Basin, while the others (JNDL-1, JNDL-3 and JNDL-4) are located in the vicinity of Domat Al-Jandal in the Tabuk Basin. Lithostratigraphical logs of the borehole cores and their stratigraphical interpretation and correlation are illustrated in Fig. 2. At both locations, the cored boreholes overlap, and correlation is easily achieved using evidence from lithology and wireline logs (and confirmed by palynological evidence reported herein). BAQA-1 and BAQA-2 cover an interval from the uppermost Tawil Formation, through the Sha'iba, Qasr, Subbat and lowermost Hammamiyat members of the Jauf Formation. JNDL-1, JNDL-3 and JNDL-4 cover an interval from the upper part of the Subbat Member of the Jauf Formation, through the Hammamiyat and Murayr members of the Jauf Formation, and into the lower part of the Jubah Formation. In total, a 1640 ft composite sequence is covered by the five cored boreholes (Fig. 2). Distribution of the samples collected and palynologically analyzed in this study is illustrated in Fig. 2 with details provided in Appendix A.

Samples from BAQA-1, BAQA-2, JNDL-3 and JNDL-4 were prepared in the Palynological Research Facility of the University of Sheffield whereas these from JNDL-1 were processed in the laboratory of '*Paléobotanique*, *Palynologie* et *Micropaléontologie*' of the University of Liège. All the 188 samples were prepared using standard palynological acid maceration techniques. The vast majority of samples were productive, yielding palynomorphs that are well preserved and of low thermal maturity (T.A.I. ca. 2). Because of the low thermal maturity, oxidation of the organic material was not required. Samples were equally subdivided between KTH/PS/CHW and logged, with PB examining the entire sequence and collating the data. All figured material is housed in the Centre for Palynology of the University, Department of Animal and Plant Sciences, University of Sheffield and in the collections of the laboratory of '*Paléobotanique*, *Palynologie* et *Micropaléontologie*', University of Liège. Individual specimens are located by providing borehole, slide details and England Finder Co-ordinates (EFC).

5. Systematic palaeontology

5.1. List of species

The identified miospore taxa are reported in the following list (in alphabetical order). Figured taxa are indicated (Plates 1–12):

Acinosporites acanthomammillatus Richardson, 1965

Acinosporites apiculatus (Streel) Streel, 1967 (Plate 4, Fig. 1)

Acinosporites lindlarensis Riegel, 1968 (Plate 4, Fig. 2)

Acinosporites spp.

Ambitisporites avitus Hoffmeister, 1959 (Plate 4, Fig. 3)

Ambitisporites eslae (Cramer and Díez) Richardson et al., 2001 (Plate 4, Fig. 4)

Amicosporites streelii Steemans, 1989 (Plate 4 Figs. 5 and 6)

Anapiculatisporites petilus Richardson, 1965 emend. McGregor and Camfield, 1982

Aneurospora goensis Lele and Streel, 1969

Aneurospora cf. *tojoides* Cramer, 1966a

Aneurospora spp.

Apiculiretusispora arenorugosa McGregor, 1973

Apiculiretusispora brandtii Streel, 1964 (Plate 4, Figs. 7 and 8)

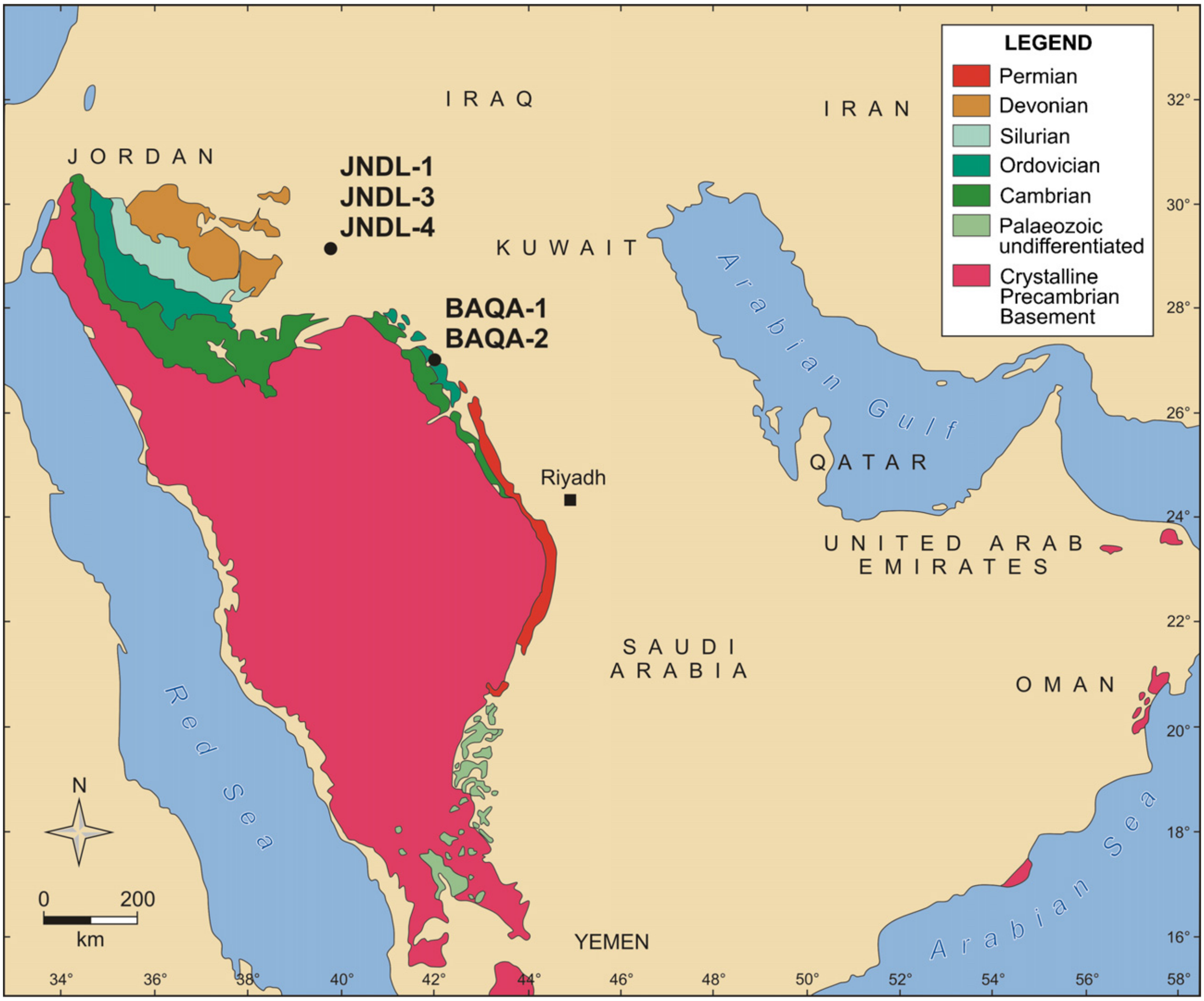

Fig. 1. Geological map of the Arabian Peninsula illustrating the location of boreholes investigated in this study.
Fig. 1. Carte géologique de la Péninsule arabique indiquant l'emplacement des forages analysés au cours de cette étude.

Apiculiretusispora plicata (Allen) Streel, 1967 (Plate 4, Fig. 9)

Apiculiretusispora spp.

Archaeozonotriletes chulus (Cramer) Richardson and Lister, 1969 (Plate 4, Figs. 10–12)

Artemopyra inconspicua nov. sp. (Plate 1, Figs. 1–5)

Artemopyra recticosta nov. sp. (Plate 1, Figs. 6–12)

Biornatispora spp.

Brochotriletes foveolatus Naumova, 1953 (Plate 4, Fig. 13)

Camarozonotriletes filatoffii nov. sp. (Plate 4, Figs. 14–23; Plate 5, Fig. 1)

Camarozonotriletes rugulosus nov. sp. (Plate 5, Figs. 2–9)

Camarozonotriletes sextantii McGregor and Camfield, 1976 (Plate 5, Fig. 10)

Chelinospora cantabrica Richardson et al., 2001

Chelinospora cf. *hemiesferica* Richardson et al., 2001

Chelinospora spp.

Cirratriradites diaphanus Steemans, 1989 (Plate 5, Fig. 11)

Clivosispora verrucata McGregor, 1973 (Plate 5, Figs. 12–14)

Cymbohilates baqaensis nov. sp. (Plate 1, Figs. 13–19)

Cymbohilates comptulus nov. sp. (Plate 2, Figs. 1–7)

Cymbohilates cymosus Richardson, 1996 (Plate 2, Fig. 8)

Cymbohilates heteroverrucosus nov. sp. (Plate 2, Figs. 9–12; Plate 3, Figs. 1 and 2)

Cymbosporites asymmetricus nov. sp. (Plate 5, Figs. 15–19; Plate 6, Figs. 1 and 2)

Cymbosporites dammamensis Steemans, 1995 (Plate 6, Figs. 3–5)

Cymbosporites? *senex* McGregor and Camfield, 1976 (Plate 6, Figs. 6 and 7)

Dibolisporites echinaceus (Eisenack) Richardson, 1965 (Plate 6, Fig. 8)

Dibolisporites eifeliensis (Lanninger) McGregor, 1973 (Plate 6, Fig. 9)

Dibolisporites pilatus nov. sp. (Plate 6, Figs. 10–13)

Dibolisporites spp.

Dictyotriletes biornatus nov. sp. (Plate 7, Figs. 1–9)

Dictyotriletes emsiensis (Allen) McGregor, 1973 (Plate 7, Figs. 10 and 11)

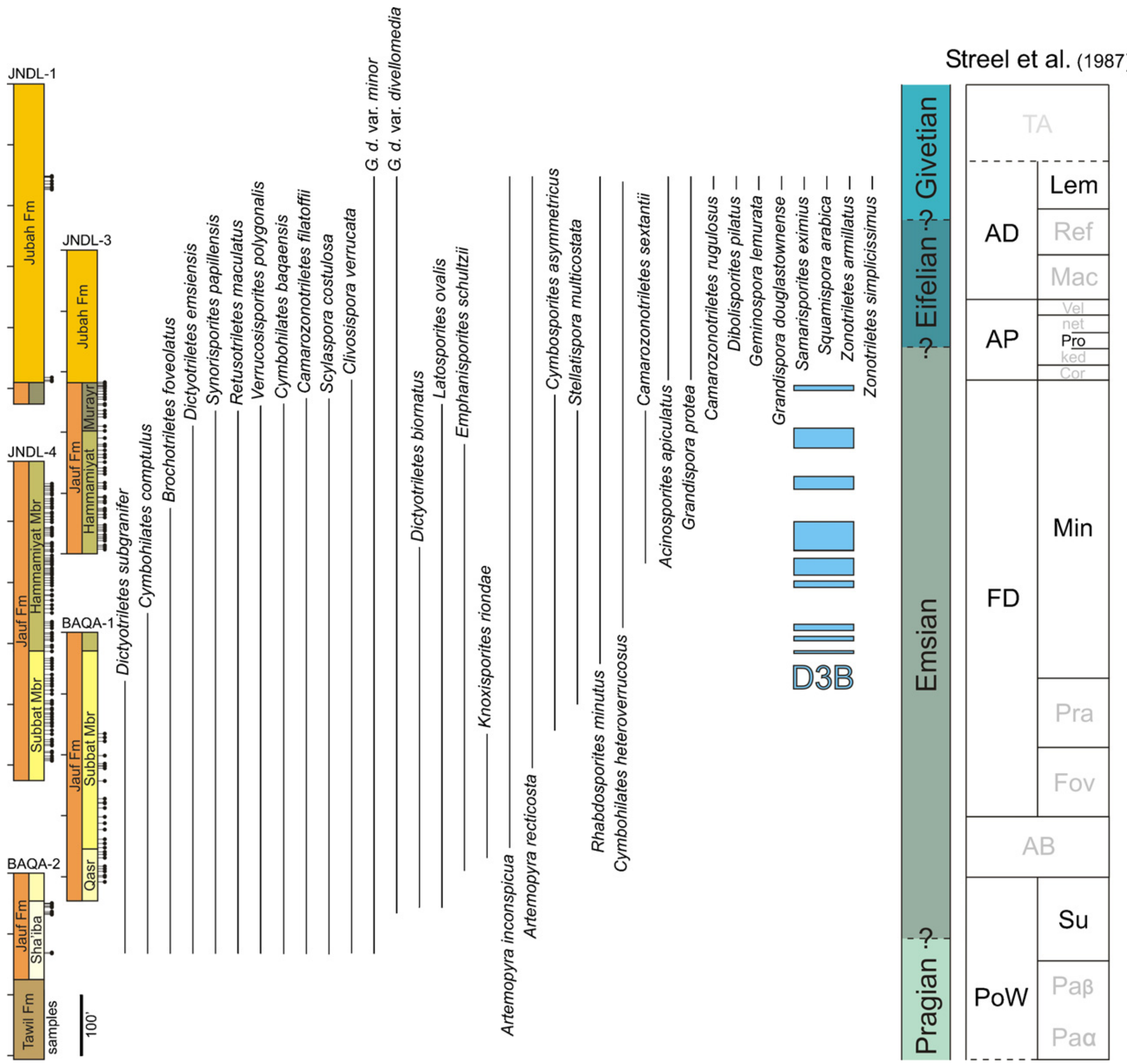

Fig. 2. Stratigraphic ranges of selected spore taxa encountered in this study compared with the west European zonation of Streel et al. (1987). The biozones that are not recognized in the study are in grey. D3B is a recurrent sphaeromorph-dominated palynosubzone of significance for regional correlations (see text for details).
Fig. 2. Distribution stratigraphique d'une sélection des spores observées au cours de l'étude et comparaisons avec la zonation ouest-européenne de Streel et al. (1987). Les biozones non identifiées au cours de l'étude sont en gris. D3B est une sous-palynozone récurrente à sphaeromorphes dominants, significative pour les corrélations régionales (voir le texte pour les détails).

Dictyotriletes favosus McGregor and Camfield, 1976

Dictyotriletes subgranifer McGregor, 1973 (Plate 7, Figs. 12 and 13)

Dictyotriletes?*gorgoneus* in McGregor, 1973 (Plate 7, Figs. 14 and 15)

Dyadaspora murusattenuata Strother and Traverse, 1979

Emphanisporites annulatus McGregor, 1961 (Plate 8, Fig. 1)

Emphanisporites decoratus Allen, 1965

Emphanisporites mcgregorii Cramer, 1967 (Plate 8, Figs. 2 and 3)

Emphanisporites rotatus McGregor emend. McGregor, 1973 (Plate 8, Fig. 4)

Emphanisporites schultzii McGregor, 1973 (Plate 8, Figs. 5 and 6)

Geminospora lemurata (Balme) Playford, 1983 (Plate 8, Figs. 7–9)

Gneudnaspora divellomedia (Chibrikova) Balme, 1988 var. *divellomedia* (Plate 3, Figs. 3–9)

Gneudnaspora divellomedia (Chibrikova) Balme, 1988 var. *minor* nov. var. (Plate 3, Figs. 10–16)

Grandispora douglastownense McGregor, 1973 (Plate 8, Fig. 10)

Grandispora protea (Naumova) Moreau-Benoît, 1976 (Plate 9, Fig. 1)

?*Knoxisporites riondae* Cramer and Díez, 1975 (Plate 9, Figs. 2 and 3)

Latosporites ovalis nov. sp. (Plate 12, Figs. 8–12)

Raistrickia spp.

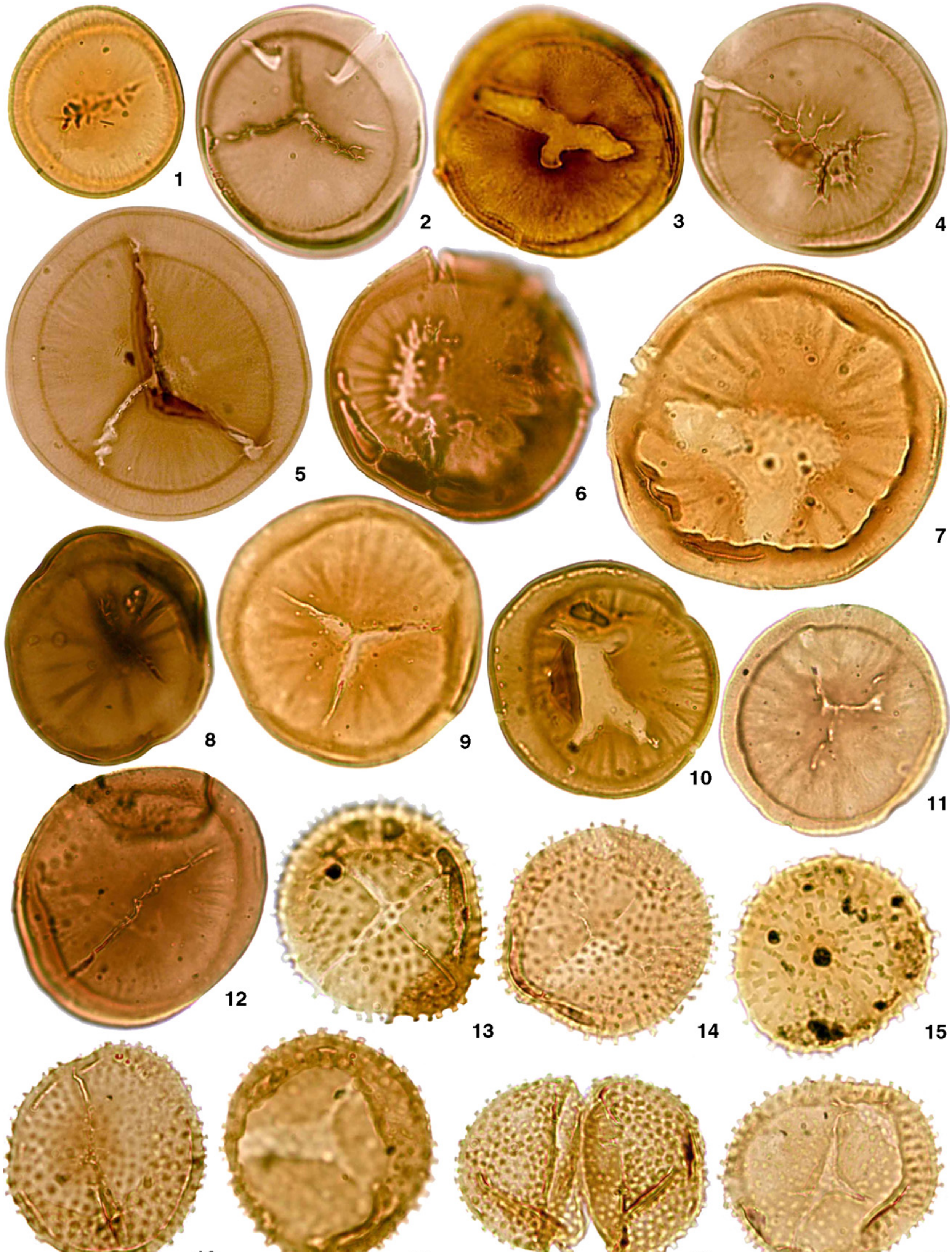

Plate 1.

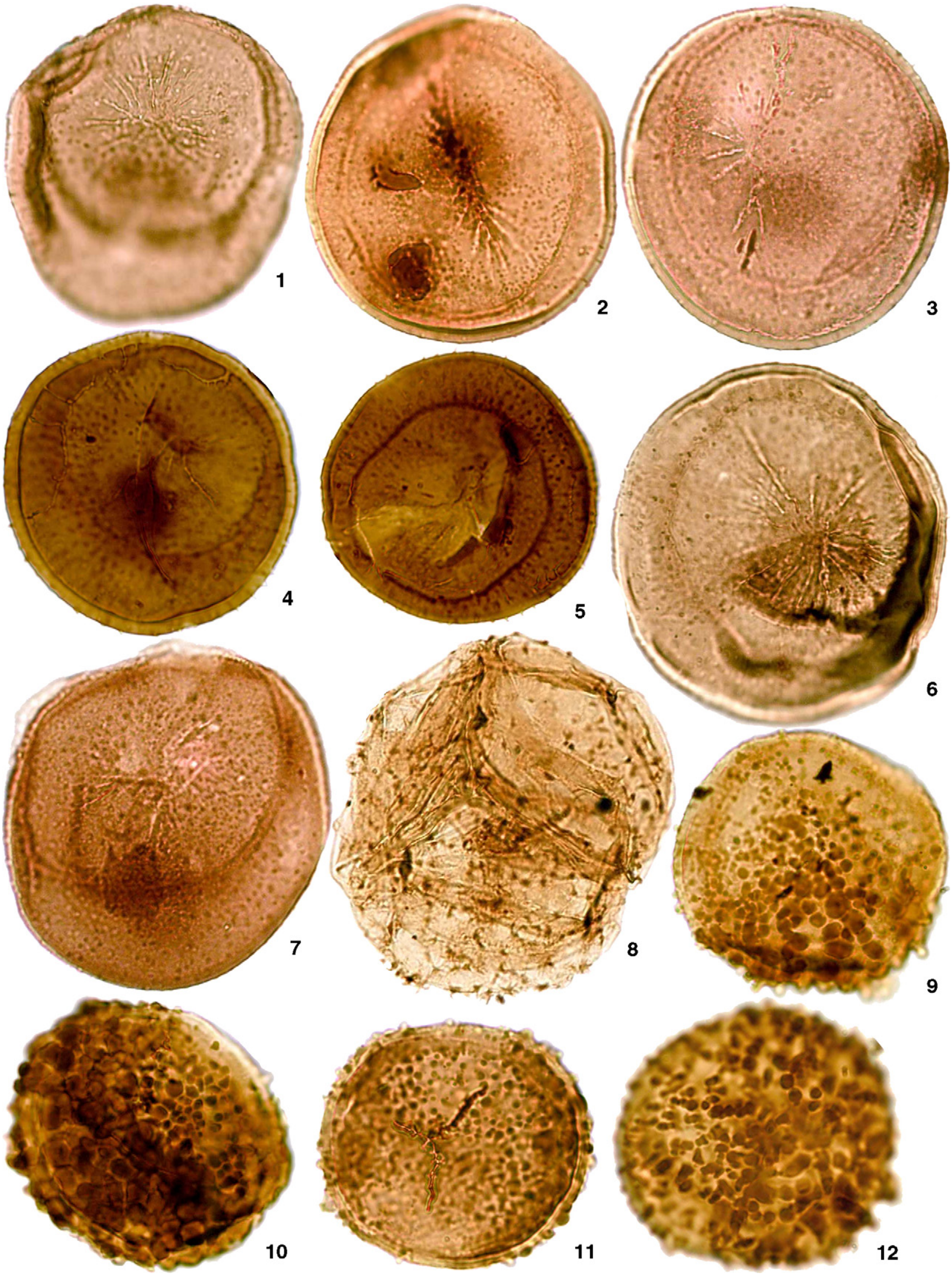

Plate 2.

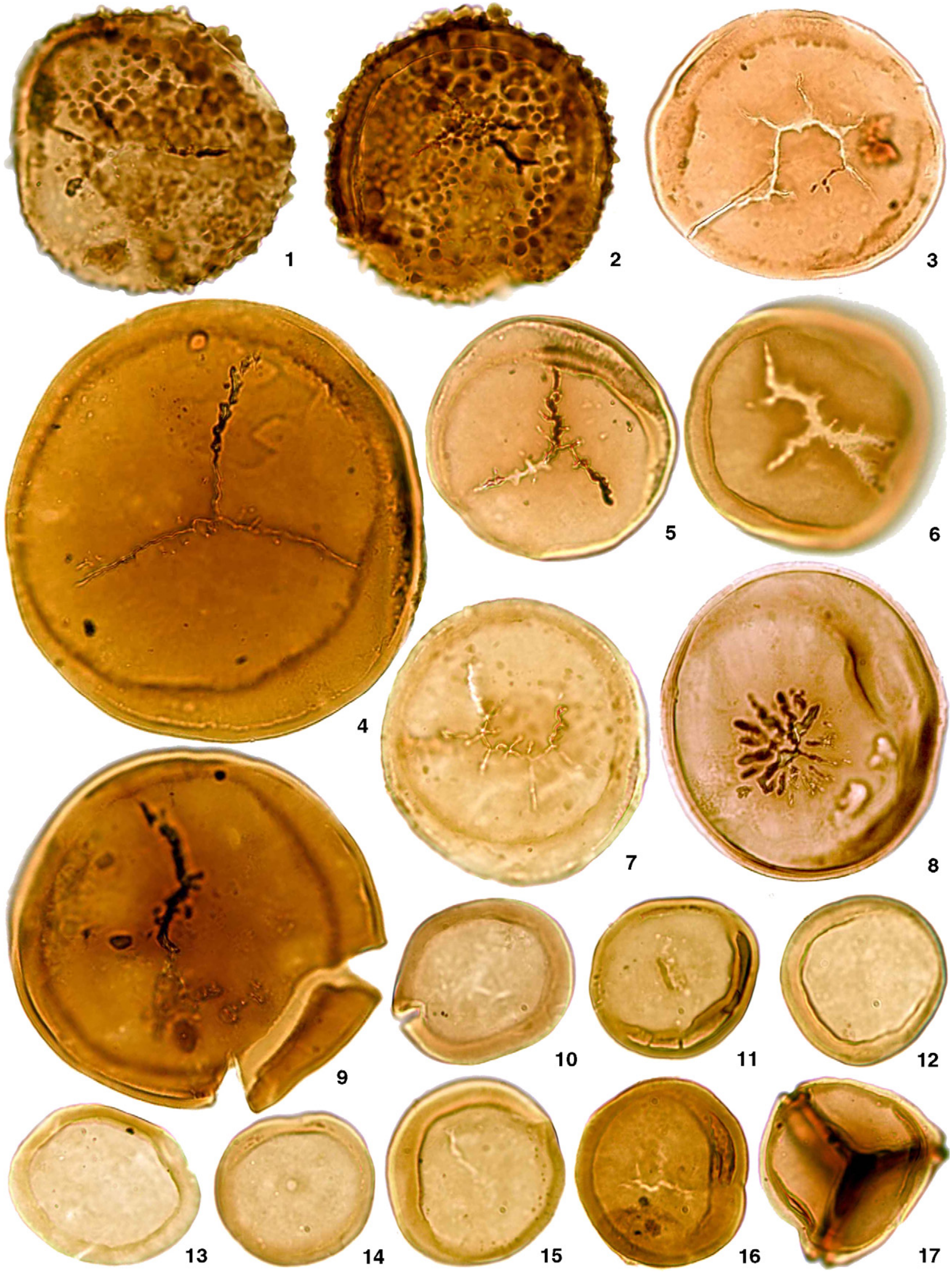

Plate 3.

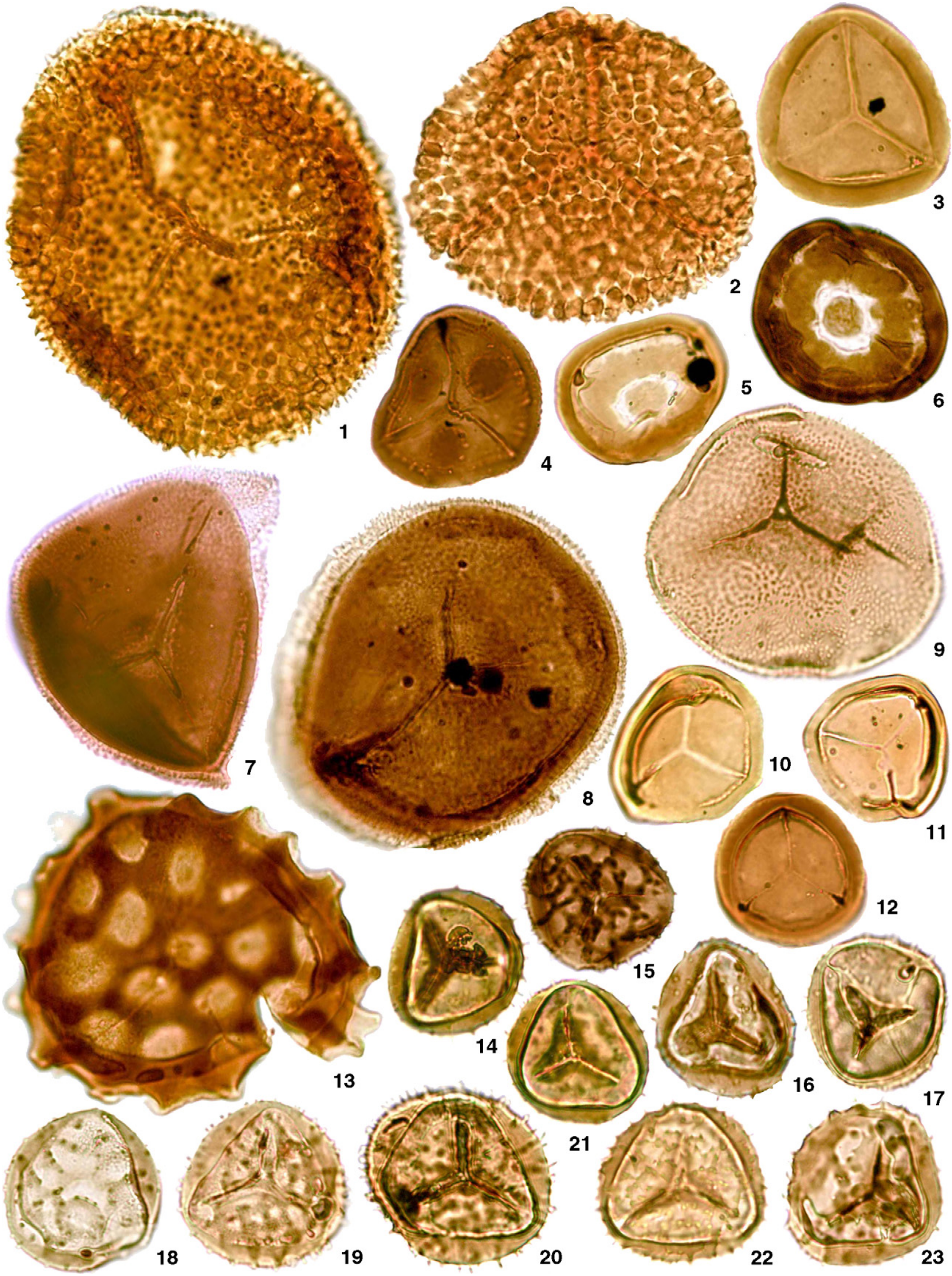

Plate 4.

Plate 5.

Plate 6.

Plate 7.

Plate 8.

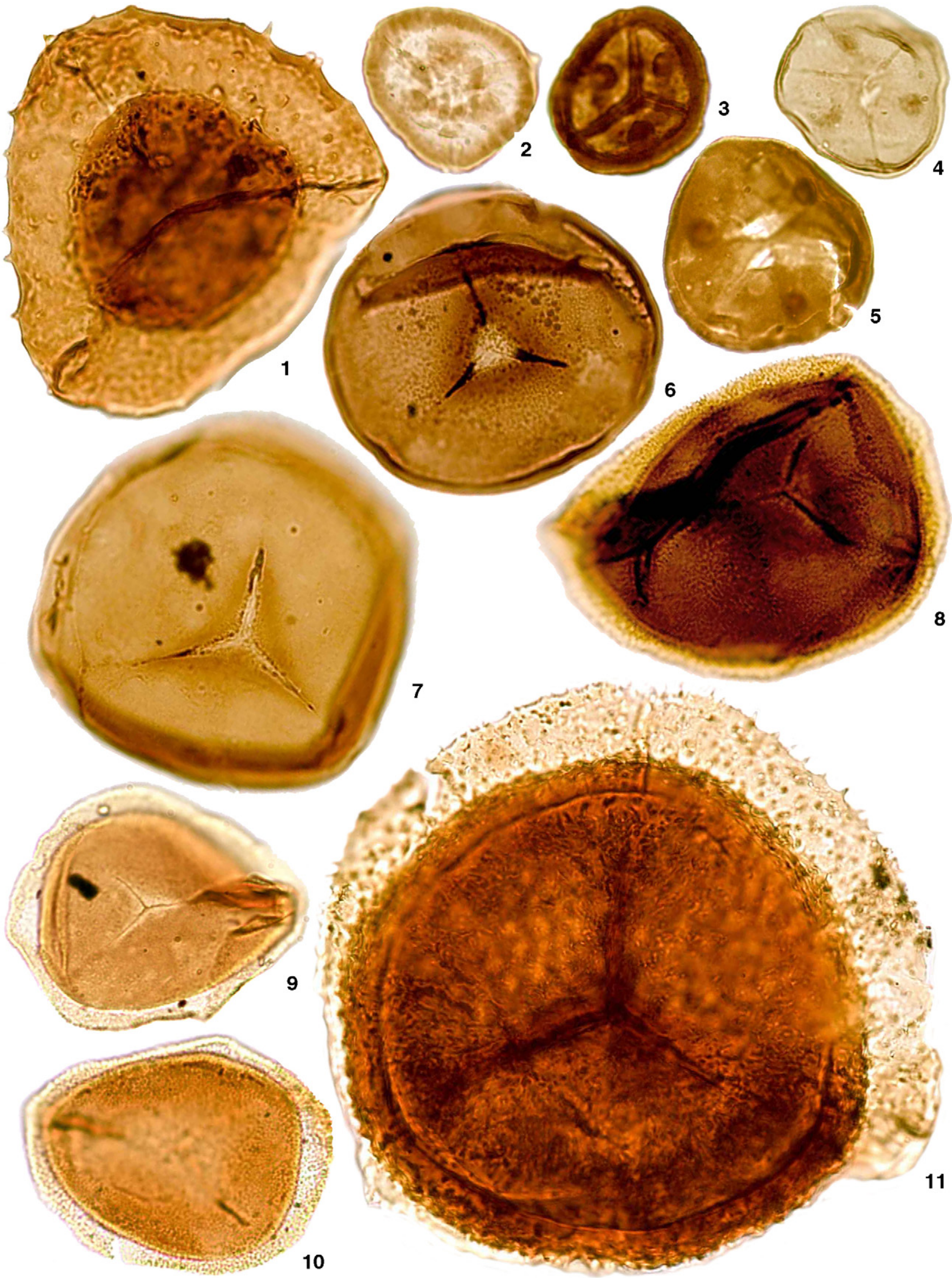

Plate 9.

Plate 1. Each miospore is identified by borehole, sample, slide numbers and England Finder Co-ordinate. Magnification × 1000. It is applicable to all plates. **Fig. 1**. *Artemopyra inconspicua* nov. sp. JNDL-1, 495.0', 60855, E38/3. **Fig. 2**. *Artemopyra inconspicua* nov. sp. BAQA-1, 227.1', 03CW110, G24/1. Holotype. Hilum exhibits a pseudo-trilete mark. **Fig. 3**. *Artemopyra inconspicua* nov. sp. JNDL-3, 368.8', 03CW160, W45. **Fig. 4**. *Artemopyra inconspicua* nov. sp. BAQA-1, 223.5', 03CW109, F35/2. Paratype. **Fig. 5**. *Artemopyra inconspicua* nov. sp. BAQA-1, 219.2', 03CW107, F43-44. Paratype. Hilum exhibits a pseudo-trilete mark. **Fig. 6**. *Artemopyra recticosta* nov. sp. BAQA-1, 219.2', 03CW107, X31/2. **Fig. 7**. *Artemopyra recticosta* nov. sp. JNDL-1, 495.0', 60854, U37/4. Holotype. **Fig. 8**. *Artemopyra recticosta* nov. sp. JNDL-3, 368.8', 03CW160, N43. Paratype. **Fig. 9**. *Artemopyra recticosta* nov. sp. JNDL-1, 156.0', 60839, U44/4. Hilum exhibits a pseudo-trilete mark that does not reach curvatura. **Fig. 10**. *Artemopyra recticosta* nov. sp. JNDL-1, 155.6', 60837, P28/2. **Fig. 11**. *Artemopyra recticosta* nov. sp. JNDL-1, 155.6', 60837, A29/4. **Fig. 12**. *Artemopyra recticosta* nov. sp. JNDL-1, 155.6', 60837, L44. **Fig. 13**. *Cymbohilates baqaensis* nov. sp. BAQA-2, 54.8', 03CW129, S44/1. Holotype. **Fig. 14**. *Cymbohilates baqaensis* nov. sp. BAQA-2, 54.8', 03CW129, Q23/4. Paratype. **Fig. 15**. *Cymbohilates baqaensis* nov. sp. BAQA-2, 54.8', 03CW129, S38/1. **Fig. 16**. *Cymbohilates baqaensis* nov. sp. BAQA-2, 50.2', 03CW126, V33/2. **Fig. 17**. *Cymbohilates baqaensis* nov. sp. BAQA-2, 50.2', 03CW126, S47/1. Paratype. **Fig. 18**. *Cymbohilates baqaensis* nov. sp. BAQA-2, 50.8', 03CW127, M28. **Fig. 19**. *Cymbohilates baqaensis* nov. sp. BAQA-2, 52.0', 03CW128, J33/1.

Planche 1. Chaque miospore est identifiée par le puits, l'échantillon, le numéro de lame et ses coordonnées England-Finder. Grossissement ×1000 pour toutes les planches. Figs. 2 et 5. Le hilum présente une pseudo-marque trilète. Fig. 9. Le hilum présente une pseudo-marque trilète qui n'atteint pas les curvatures.

Plate 2. **Fig. 1**. *Cymbohilates comptulus* nov. sp. BAQA-1, 222.5', 03CW108, Y35. **Fig. 2**. *Cymbohilates comptulus* nov. sp. BAQA-1, 205.8', 03CW106, N50/2. **Fig. 3**. *Cymbohilates comptulus* nov. sp. BAQA-1, 205.8', 03CW106, W25. Holotype. **Fig. 4**. *Cymbohilates comptulus* nov. sp. BAQA-1, 285.5', 03CW111, V30. **Fig. 5**. *Cymbohilates comptulus* nov. sp. BAQA-1, 285.5', 03CW111, W31. **Fig. 6**. *Cymbohilates comptulus* nov. sp. BAQA-1, 222.5', 03CW108, P48. Paratype. **Fig. 7**. *Cymbohilates comptulus* nov. sp. BAQA-1, 205.8', 03CW106, O23/1. Paratype. **Fig. 8**. *Cymbohilates cymosus* Richardson, 1996. BAQA-2, 134.4', 03CW137, M34/2. Permanent tetrad. **Fig. 9**. *Cymbohilates heteroverrucosus* nov. sp. JNDL-1, 172.7', 60845, L28. Holotype. **Fig. 10**. *Cymbohilates heteroverrucosus* nov. sp. JNDL-1, 167.8', 60843, D27/3. **Fig. 11**. *Cymbohilates heteroverrucosus* nov. sp. JNDL-1, 174.6', 60847, E33/1. **Fig. 12**. *Cymbohilates heteroverrucosus* nov. sp. JNDL-1, 177.0', 60850, P48/1.

Plate 3. **Fig. 1**. *Cymbohilates heteroverrucosus* nov. sp. JNDL-1, 177.0', PPM009, G33. **Fig. 2**. *Cymbohilates heteroverrucosus* nov. sp. JNDL-1, 177.0', 60849, H44. Paratype. **Fig. 3**. *Gneudnaspora divellomedia* (Chibrikova) Balme, 1988 var. *divellomedia*. JNDL-1, 167.8', PPM006, Q36/3. **Fig. 4**. *Gneudnaspora divellomedia* (Chibrikova) Balme, 1988 var. *divellomedia*. JNDL-1, 156.0', 60839, U32/1. Hilum exhibits a pseudo-trilete mark. **Fig. 5**. *Gneudnaspora divellomedia* (Chibrikova) Balme, 1988 var. *divellomedia*. JNDL-1, 156.0', PPM004, C45. **Fig. 6**. *Gneudnaspora divellomedia* (Chibrikova) Balme, 1988 var. *divellomedia*. JNDL-1, 155.6', 60837, M27. **Fig. 7**. *Gneudnaspora divellomedia* (Chibrikova) Balme, 1988 var. *divellomedia*. JNDL-1, 174.6', PPM008, U31. **Fig. 8**. *Gneudnaspora divellomedia* (Chibrikova) Balme, 1988 var. *divellomedia*. BAQA-1, 219.2', 03CW107, G49. **Fig. 9**. *Gneudnaspora divellomedia* (Chibrikova) Balme, 1988 var. *divellomedia*. JNDL-4, 52.3', 03CW188, V26. **Fig. 10**. *Gneudnaspora divellomedia* (Chibrikova) Balme, 1988 var. *minor* nov. var. BAQA-2, 57.2', 03CW131, E25/4. **Fig. 11**. *Gneudnaspora divellomedia* (Chibrikova) Balme, 1988 var. *minor* nov. var. BAQA-2, 50.2', 03CW126, V30. **Fig. 12**. *Gneudnaspora divellomedia* (Chibrikova) Balme, 1988 var. *minor* nov. var. BAQA-2, 54.8', 03CW129, G49. Paratype. **Fig. 13**. *Gneudnaspora divellomedia* (Chibrikova) Balme, 1988 var. *minor* nov. var. JNDL-1, 172.7', PPM007, M49/3. **Fig. 14**. *Gneudnaspora divellomedia* (Chibrikova) Balme, 1988 var. *minor* nov. var. BAQA-2, 52.0', 03CW128, T32/3. **Fig. 15**. *Gneudnaspora divellomedia* (Chibrikova) Balme, 1988 var. *minor* nov. var. BAQA-2, 50.2', 03CW126, B49/2. Holotype. **Fig. 16**. *Gneudnaspora divellomedia* (Chibrikova) Balme, 1988 var. *minor* nov. var. BAQA-2, 50.8', 03CW127, L38/1. **Fig. 17**. *Tetrahedraletes medinensis* Strother and Traverse, 1979. JNDL-1, 156.0', 60840, F43/4.

Plate 4. **Fig. 1**. *Acinosporites apiculatus* (Streel) Streel, 1967. JNDL-1, 495.0', PPM014, O29. **Fig. 2**. *Acinosporites lindlarensis* Riegel, 1968. JNDL-1, 162.3', PPM005, P37/4. **Fig. 3**. *Ambitisporites avitus* Hoffmeister, 1959. BAQA-2, 52.0', 03CW128, O47/1. **Fig. 4**. *Ambitisporites eslae* (Cramer and Díez) Richardson et al., 2001. BAQA-1, 371.1', 03CW118, V36/3. **Fig. 5**. *Amicosporites streelii* Steemans, 1989. BAQA-1, 395.2', 03CW121, G26/3. **Fig. 6**. *Amicosporites streelii* Steemans, 1989. BAQA-1, 285.5', 03CW111, V44. **Fig. 7**. *Apiculiretusispora brandtii* Streel, 1964. BAQA-1, 219.2', 03CW107, U26/2. **Fig. 8**. *Apiculiretusispora brandtii* Streel, 1964. BAQA-1, 223.5', 03CW109, V30. **Fig. 9**. *Apiculiretusispora plicata* (Allen) Streel, 1967. BAQA-1, 222.5', 03CW108, U26. **Fig. 10**. *Archaeozonotriletes chulus* (Cramer) Richardson and Lister, 1969. JNDL-1, 162.3', 60841, N32/2. **Fig. 11**. *Archaeozonotriletes chulus* (Cramer) Richardson and Lister, 1969. JNDL-1, 162.3', 60841, H45/3. **Fig. 12**. *Archaeozonotriletes chulus* (Cramer) Richardson and Lister, 1969. BAQA-2, 133.0', 03CW136, Q25/1. **Fig. 13**. *Brochotriletes foveolatus* Naumova, 1953. BAQA-1, 223.5', 03CW109, T23/2. **Fig. 14**. *Camarozonotriletes filatoffii* nov. sp. BAQA-1, 223.5', 03CW109, S48/4. **Fig. 15**. *Camarozonotriletes filatoffii* nov. sp. BAQA-1, 285.5', 03CW111, N51/2. **Fig. 16**. *Camarozonotriletes filatoffii* nov. sp. BAQA-1, 223.5', 03CW109, N45/2. **Fig. 17**. *Camarozonotriletes filatoffii* nov. sp. BAQA-1,.223.5', 03CW109, N24. **Fig. 18**. *Camarozonotriletes filatoffii* nov. sp. BAQA-1, 219.2', 03CW107, V39/1. **Fig. 19**. *Camarozonotriletes filatoffii* nov. sp. BAQA-1, 222.5', 03CW108, W30. Paratype. **Fig. 20**. *Camarozonotriletes filatoffii* nov. sp. BAQA-1, 222.5', 03CW108, V44/4. **Fig. 21**. *Camarozonotriletes filatoffii* nov. sp. BAQA-1, 223.5', 03CW109, M37. Paratype. **Fig. 22**. *Camarozonotriletes filatoffii* nov. sp. BAQA-2, 133.0', 03CW136, H25. Holotype. **Fig. 23**. *Camarozonotriletes filatoffii* nov. sp. BAQA-1, 227.1', 03CW110, Q47.

Plate 5. **Fig. 1**. *Camarozonotriletes filatoffii* nov. sp. BAQA-1, 222.5', 03CW108, J-K36. Tetrad. **Fig. 2**. *Camarozonotriletes rugulosus* nov. sp. JNDL-1, 156.0', 60840, T48. Holotype. **Fig. 3**. *Camarozonotriletes rugulosus* nov. sp. JNDL-1, 167.8', 60842, G51/4. **Fig. 4**. *Camarozonotriletes rugulosus* nov. sp. JNDL-1, 156.0', 60839, M49/3. Paratype. **Fig. 5**. *Camarozonotriletes rugulosus* nov. sp. JNDL-1, 156.0', PPM004, J41/4. **Fig. 6**. *Camarozonotriletes rugulosus* nov. sp. JNDL-1, 172.7', 60846, P46/2. Paratype. **Fig. 7**. *Camarozonotriletes rugulosus* nov. sp. JNDL-1, 155.6', 60838, J42/2. **Fig. 8**. *Camarozonotriletes rugulosus* nov. sp. JNDL-1, 174.6', PPM008, L-M44. **Fig. 9**. *Camarozonotriletes rugulosus* nov. sp. JNDL-1, 172.7', PPM007, C47/4. **Fig. 10.** *Camarozonotriletes sextantii* McGregor and Camfield, 1976. JNDL-4, 75.0', 03CW192, E32/1. **Fig. 11**. *Cirratriradites diaphanus* Steemans, 1989. BAQA-2, 50.2', 03CW126, B45. **Fig. 12**. *Clivosispora verrucata* McGregor, 1973. BAQA-1, 222.5', 03CW108, M-N26. **Fig. 13**. *Clivosispora verrucata* McGregor, 1973. BAQA-1, 395.2', 03CW121, F47/1. **Fig. 14**. *Clivosispora verrucata* McGregor, 1973. BAQA-1, 285.5', 03CW111, U35. **Fig. 15**. *Cymbosporites asymmetricus* nov. sp. JNDL-3, 413.2', 03CW166, C40. **Fig. 16**. *Cymbosporites asymmetricus* nov. sp. JNDL-4, 160.7', 03CW211, V42. Paratype. **Fig. 17**. *Cymbosporites asymmetricus* nov. sp. JNDL-4, 214.3', 03CW226, X52. This specimen displays a local slight detachment of the exospore. **Fig. 18**. *Cymbosporites asymmetricus* nov. sp. JNDL-4, 214.3', 03CW111, V51. **Fig. 19**. *Cymbosporites asymmetricus* nov. sp. JNDL-4, 42.0', 03CW186, R48.

Plate 6. **Fig. 1**. *Cymbosporites asymmetricus* nov. sp. JNDL-3, 413.2', 03CW166, T42/1. Holotype. **Fig. 2**. *Cymbosporites asymmetricus* nov. sp. JNDL-3, 368.8', 03CW160, L49. **Fig. 3**. *Cymbosporites dammamensis* Steemans, 1995. BAQA-2, 133.0', 03CW136, R26/2. **Fig. 4**. *Cymbosporites dammamensis* Steemans, 1995. BAQA-2, 134.4', 03CW137, N42. **Fig. 5**. *Cymbosporites dammamensis* Steemans, 1995. BAQA-1, 371.1', 03CW118, T54. **Fig. 6**. *Cymbosporites*? *senex* McGregor and Camfield, 1976. BAQA-1, 285.5', 03CW111, W44/1. **Fig. 7**. *Cymbosporites*? *senex* McGregor and Camfield, 1976. JNDL-1, 495.0', 60855, O30. **Fig. 8**. *Dibolisporites echinaceus* (Eisenack) Richardson, 1965. BAQA-2, 50.8', 03CW127, P25/3. **Fig. 9**. *Dibolisporites eifeliensis* (Lanninger) McGregor, 1973. BAQA-2, 134.4', 03CW137, J30/1. **Fig. 10**. *Dibolisporites pilatus* nov. sp. JNDL-1, 177.0', PPM009, N39. **Fig. 11**. *Dibolisporites pilatus* nov. sp. JNDL-1, 167.8', PPM006, V48. Holotype. **Fig. 12**. *Dibolisporites pilatus* nov. sp. JNDL-1, 174.6', 60847, M29/3. **Fig. 13**. *Dibolisporites pilatus* nov. sp. JNDL-1, 167.8', 60842, R42/3. Paratype.

Plate 7. **Fig. 1**. *Dictyotriletes biornatus* nov. sp. BAQA-1, 308.3', 03CW112, E48/2. **Fig. 2**. *Dictyotriletes biornatus* nov. sp. JNDL-4, 448.6', 03CW267, U33/2. **Fig. 3**. *Dictyotriletes biornatus* nov. sp. BAQA-1, 366.9', 03CW117, L27/1. Paratype. **Fig. 4**. *Dictyotriletes biornatus* nov. sp. JNDL-4, 448.6', 03CW267, H34/3. A branch of the trilete mark is visible. **Fig. 5**. *Dictyotriletes biornatus* nov. sp. BAQA-1, 345.5', 03CW114, O53. Holotype. **Fig. 6**. *Dictyotriletes biornatus* nov. sp. JNDL-4, 495.2', 03CW275, L41/4. **Fig. 7**. *Dictyotriletes biornatus* nov. sp. JNDL-4, 464.1', 03CW269, M37/1. **Fig. 8**. *Dictyotriletes biornatus* nov. sp. BAQA-1, 219.2', 03CW107, L40/4. Paratype. **Fig 9**. *Dictyotriletes biornatus* nov. sp. BAQA-1, 169.1', 03CW103, K26. **Fig. 10**. *Dictyotriletes emsiensis* (Allen) McGregor, 1973. BAQA-2, 56.0', 03CW128, X46. **Fig. 11**. *Dictyotriletes emsiensis* (Allen) McGregor, 1973. BAQA-2, 134.4', 03CW137, Q29/3. **Fig. 12**. *Dictyotriletes subgranifer* McGregor, 1973. BAQA-1, 366.9', 03CW117, O31. **Fig. 13**. *Dictyotriletes subgranifer* McGregor, 1973. BAQA-2, 134.4', 03CW137, T39/2. **Fig. 14**. *Dictyotriletes?gorgoneus* in McGregor, 1973. BAQA-2, 50.8', 03CW127, G54. **Fig. 15**. *Dictyotriletes?gorgoneus* in McGregor, 1973. BAQA-2, 50.8', 03CW267, D24.

Plate 8. **Fig. 1**. *Emphanisporites annulatus* McGregor, 1961. JNDL-1, 172.7', 60846, S30/2. **Fig. 2**. *Emphanisporites mcgregorii* Cramer, 1967. JNDL-1, 177.0', PPM009, K47/3. **Fig. 3**. *Emphanisporites mcgregorii* Cramer, 1967. BAQA-2, 134.4', 03CW137, E52. **Fig. 4**. *Emphanisporites rotatus* McGregor emend. McGregor, 1973. BAQA-1, 345.5', 03CW114, H50/1. **Fig. 5**. *Emphanisporites schultzii* McGregor, 1973. BAQA-1, 395.2', 03CW121, G50. **Fig. 6**. *Emphanisporites schultzii* McGregor, 1973. JNDL-4, 182.5', 03CW220, R38. Incomplete tetrad. **Fig. 7**. *Geminospora lemurata* (Balme) Playford, 1983. JNDL-1, 172.7', PPM007, O49/3. **Fig. 8**. *Geminospora lemurata* (Balme) Playford, 1983. JNDL-1, 167.8', 60842, E34. **Fig. 9**. *Geminospora lemurata* (Balme) Playford, 1983. JNDL-1, 162.3', 60841, G30/2. **Fig. 10**. *Grandispora douglastownense* McGregor, 1973. JNDL-1, 177.0', 60850, P45/4.

Plate 9. **Fig. 1**. *Grandispora protea* (Naumova) Moreau-Benoît, 1976. JNDL-1, 156.0', PPM004, H44/4. **Fig. 2.** ?*Knoxisporites riondae* Cramer and Díez, 1975. BAQA-1, 285.5', 03CW111, R48/3. **Fig. 3**. ?*Knoxisporites riondae* Cramer and Díez, 1975. BAQA-1, 366.9', 03CW117, M32/2. **Fig. 4**. *Retusotriletes maculatus* McGregor and Camfield, 1976. BAQA-1, 219.2', 03CW107, F35. **Fig. 5**. *Retusotriletes maculatus* McGregor and Camfield, 1976. BAQA-1, 285.5', 03CW111, Q34. **Fig. 6**. *Retusotriletes rotundus* (Streel) Lele and Streel, 1969. BAQA-1, 371.1', 03CW118, P33. **Fig. 7**. *Retusotriletes triangulatus* (Streel) Streel, 1967. BAQA-1, 345.5', 03CW114, M35/1. **Fig. 8**. *Rhabdosporites minutus* Tiwari and Schaarschmidt, 1975. JNDL-3, 368.8', 03CW160, H45/1. **Fig. 9**. *Rhabdosporites minutus* Tiwari and Schaarschmidt, 1975. JNDL-1, 177.0', PPM009, U32. **Fig. 10**. *Rhabdosporites minutus* Tiwari and Schaarschmidt, 1975. JNDL-1, 156.0', 60839, S36. **Fig. 11**. *Samarisporites eximius* (Allen) Loboziak and Streel, 1989. JNDL-1, 162.3', PPM005, S45/3.

Retusotriletes maculatus McGregor and Camfield, 1976 (Plate 9, Figs. 4 and 5)

Retusotriletes rotundus (Streel) Lele and Streel, 1969 (Plate 9, Fig. 6)

Retusotriletes triangulatus (Streel) Streel, 1967 (Plate 9, Fig. 7)

Retusotriletes spp.

Rhabdosporites minutus Tiwari and Schaarschmidt, 1975 (Plate 9, Figs. 8–10)

Samarisporites eximius (Allen) Loboziak and Streel, 1989 (Plate 9, Fig. 11)

Scylaspora costulosa nov. sp. (Plate 10, Figs. 1–5)

Squamispora arabica nov. gen. et sp. (Plate 10, Figs. 6–10)

Stellatispora multicostata nov. sp. (Plate 11, Figs. 1–4)

Synorisporites papillensis McGregor, 1973 (Plate 11, Figs. 5 and 6)

Tetrahedraletes medinensis Strother and Traverse, 1979 (Plate 3, Fig. 17)

Verruciretusispora dubia (Eisenack) Richardson and Rasul, 1978

Verrucosisporites flexibilis Turnau, 1986

Verrucosisporites polygonalis Lanninger, 1968 (Plate 11, Fig. 7)

Verrucosisporites spp.

Zonotriletes armillatus nov. sp. (Plate 11, Figs. 8–12; Plate 12, Figs. 1 and 2)

Zonotriletes simplicissimus nov. sp. (Plate 12, Figs. 3–7)

Zonotriletes spp.

5.2. Systematic descriptions

New taxa of cryptospores, trilete spores and monolete spores are described below. Within each group, taxonomic descriptions are arranged alphabetically by genus and species.

5.2.1. Hilate cryptospores

Genus ***Artemopyra*** Burgess and Richardson emend. Richardson, 1996

Type species: *Artemopyra brevicosta* Burgess and Richardson, 1991.

Artemopyra inconspicua nov. sp.

Plate 1, Figs. 1–5

Derivation of name: Refers to the characteristics of the muri; *inconspicuus* = not well visible (Latin).

Holotype: Plate 1, Fig. 2, borehole BAQA-1, sample 227.1', slide 03CW110, EFC G24-1.

Paratypes: Plate 1, Fig. 4, borehole BAQA-1, sample 223.5', slide 03CW109, EFC F35-2. Plate 1, Fig. 5, borehole BAQA-1, sample 219.2', slide 03CW107, EFC F43-44.

Diagnosis: A distally laevigate *Artemopyra*. Hilum sculptured with weakly defined, radially disposed, straight muri, extending from the curvatura for between half to all of the way to the proximal pole.

Description: Amb circular to sub-circular. A diffuse to clear curvatura delimits a more or less circular hilum. Proximal surface is characterized by scars which often resemble a trilete mark. The hilum radius commonly equals to 3/4 to 4/5 of the amb radius. Hilum sculptured with closely spaced, radially disposed muri which are straight, 0.5–1 μm wide and 0.5–1 μm apart at the equator, becoming thinner towards the proximal pole. Typically the muri are weakly defined and extend from the curvatura for half to all of the way to the proximal pole. There are numerous muri, usually between 60 and 90. Distal surface laevigate.

Dimensions: 36 (48) 57 μm, 20 specimens measured.

Comparison: *Artemopyra brevicosta* Burgess and Richardson, 1991 has more robust, radial muri which always are confined to the equatorial region of the contact area. *Artemopyra recticosta* nov. sp. possesses thicker muri which are less numerous (18–46). *Artemopyra inconspicua* nov. sp. sometimes can be mistaken for *Gneudnaspora divellomedia* (Chibrikova) Balme, 1988 var. *divellomedia* because of the inconspicuous nature of the muri.

Occurrence: Boreholes BAQA-1 and JNDL-1, 3, 4. Jauf and Jubah formations. Emsian-Givetian.

Artemopyra recticosta nov. sp.

Plate 1, Figs. 6–12

?1986. Emphanisporites orbicularis – Turnau, p. 345, Plate 4, Figs. 4 and 9.

2007. *Artemopyra*? spp. – Wellman Plate 20, Fig. i.

Derivation of name: Refers to the straight muri; *rectus* = straight, *costa* = rib (Latin).

Holotype: Plate 1, Fig. 7, borehole JNDL-1, sample 495.0', slide 60854, EFC U37/4.

Paratype: Plate 1, Fig. 8, borehole JNDL-3, sample 368.8', slide 03CW160, EFC N43.

Diagnosis: A distally laevigate *Artemopyra*. Hilum sculptured with radially disposed, straight muri extending from the curvatura for between half to all of the way to the proximal pole.

Description: Amb circular to sub-circular. A diffuse to clear curvatura 0.6–2 μm wide delimits a more or less circular hilum. Proximal surface is characterized by different types of scars which sometimes show a shape similar to a trilete mark. The hilum radius equals or is more or less 4/5 of the amb radius. Hilum sculptured by radially disposed muri which are straight and up 0.7–2.6 μm wide at the equator, becoming thinner towards the proximal pole. They extend from the curvatura for half to all of the way to the proximal pole. There are usually 18–46 muri. Distal surface laevigate.

Dimensions: 34 (51) 70 μm, 36 specimens measured.

Comparison: *Artemopyra laevigata* Wellman and Richardson, 1996 is generally smaller (33–48 μm) and possesses proximal radial muri which are highly variable in appearance and sometimes bifurcate. *Artemopyra brevicosta* Burgess and Richardson, 1991 is smaller (22–49 μm) and shows proximal radial muri which can be slightly sinuous and are short, less than 1/2 of the hilum radius. *Emphanisporites orbicularis* Turnau, 1986 represents probably the same taxon, although this is described as a trilete spore? *Artemopyra* spp. in Wellman (2007) represents the same species described here. The trilete spore *Emphanisporites rotatus* McGregor emend. McGregor, 1973 has the same kind of muri as *Artemopyra recticosta* nov. sp.

Remark: Some specimens of *Artemopyra recticosta* nov. sp. in our material possess a darkened area which is located at or near the proximal pole.

Occurrence: Boreholes BAQA-1 and JNDL-1, 3, 4. Jauf (Subbat-Murayr members) and Jubah formations. Emsian-Givetian.

Genus ***Cymbohilates*** Richardson, 1996 emend.

Type species: *Cymbohilates horridus* Richardson, 1996.

Emended diagnosis: Proximally hilate cryptospore monads. Exospore, sculptured subequatorially and distally with grana, coni, spinae, bacula, verrucae or biform elements, sometimes fused in groups. Contact area (hilum) sculptured or smooth, with random or concentric folds, and/or radial muri. Hilum, more or less circular, curvatural ridge distinct or barely perceptible.

Remark: The diagnosis is enlarged to include either subequatorially and distally or wholly sculptured forms. The discrete positive elements can be of all types.

Cymbohilates baqaensis nov. sp.

Plate 1, Figs. 13–19

Derivation of name: Refers to the locality where this species was found; *baqaensis* = from the locality of Baq'a in Saudi Arabia (Latin).

Holotype: Plate 1, Fig. 13, borehole BAQA-2, sample 54.8', slide 03CW129, EFC S44/1.

Paratypes: Plate 1, Fig. 14, borehole BAQA-2, sample and slide 54.8', slide 03CW129, EFC Q23/4. Plate 1, Fig. 17, borehole BAQA-2, sample 50.2', slide 03CW126, EFC S47/1.

Diagnosis: A *Cymbohilates* with small bacula. The proximal surface possesses different types of scars which sometimes have a shape similar to a trilete mark.

Description: Amb circular to sub-circular. An undulating and irregular curvatura delimits a more or less circular, smooth hilum. The smooth proximal surface shows different types of scars such as multiple radial branches, cross fractures, pseudo-trilete mark, or simple slit. Exospore is sculptured subequatorially and distally with evenly distributed bacula 0.75–2 μm high, 0.75–1.5 μm wide at base and 1.5–3 μm apart. The tops of elements are flat or slightly concave, with generally bifurcate shape.

Dimensions: 30 (36) 40 μm, 16 specimens measured.

Comparison: *Cymbosporites baculatus* Turnau et al., 2005 also possesses bacula but without bifurcate shape. According to Turnau (pers. comm.), this taxon is different but is probably related. *Cymbosporites dammamensis* Steemans, 1995 appears very similar but is a trilete miospore, although its trilete mark is not always clearly perceptible. Some specimens have probably been misinterpreted in Steemans (1995) and have to be revised.

Remark: Some specimens can be preserved as dyads.

Occurrence: Boreholes BAQA-1, 2 and JNDL-3, 4. Jauf Formation (Sha'iba-Murayr members). Pragian-Emsian.

Cymbohilates comptulus nov. sp.

Plate 2, Figs. 1–7

?1988. *Gneudnaspora* sp. (Chibrikova) – Balme, p. 17, Plate 3, Fig. 15.

Derivation of name: Refers to the fine ornamentation of the distal surface; *comptulus* = finely decorated (Latin).

Holotype: Plate 2, Fig. 3, borehole BAQA-1, sample 205.8', slide 03CW106, EFC W25.

Paratypes: Plate 2, Fig. 6, borehole BAQA-1, sample 222.5', slide 03CW108, EFC P48. Plate 2, Fig. 7, borehole BAQA-1, sample 205.8', slide 03CW106, EFC O23/1.

Diagnosis: A *Cymbohilates* with small bacula, spinae and coni sparsely distributed. The proximal surface often possesses narrow radial scars in the exospore.

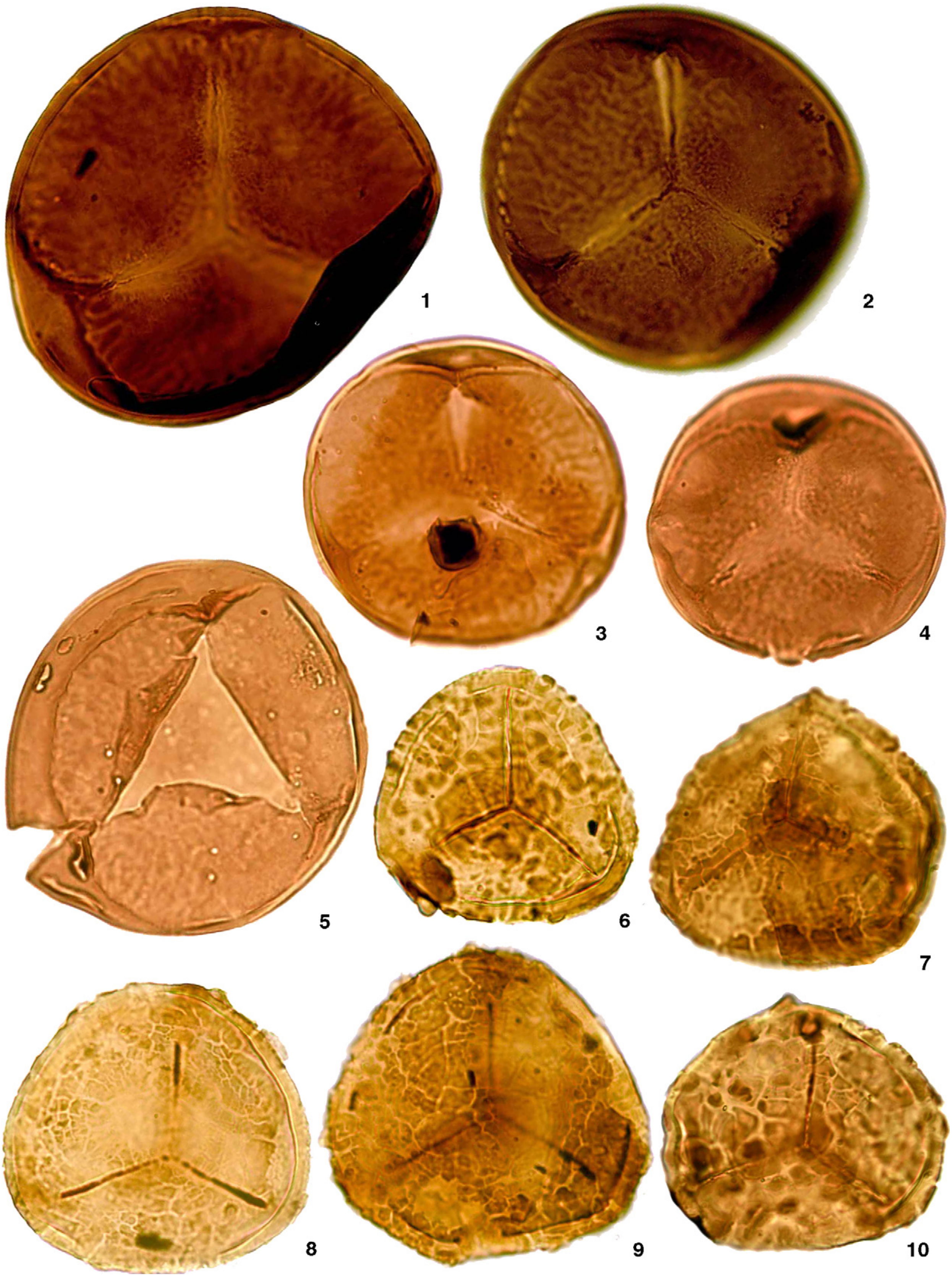

Plate 10.

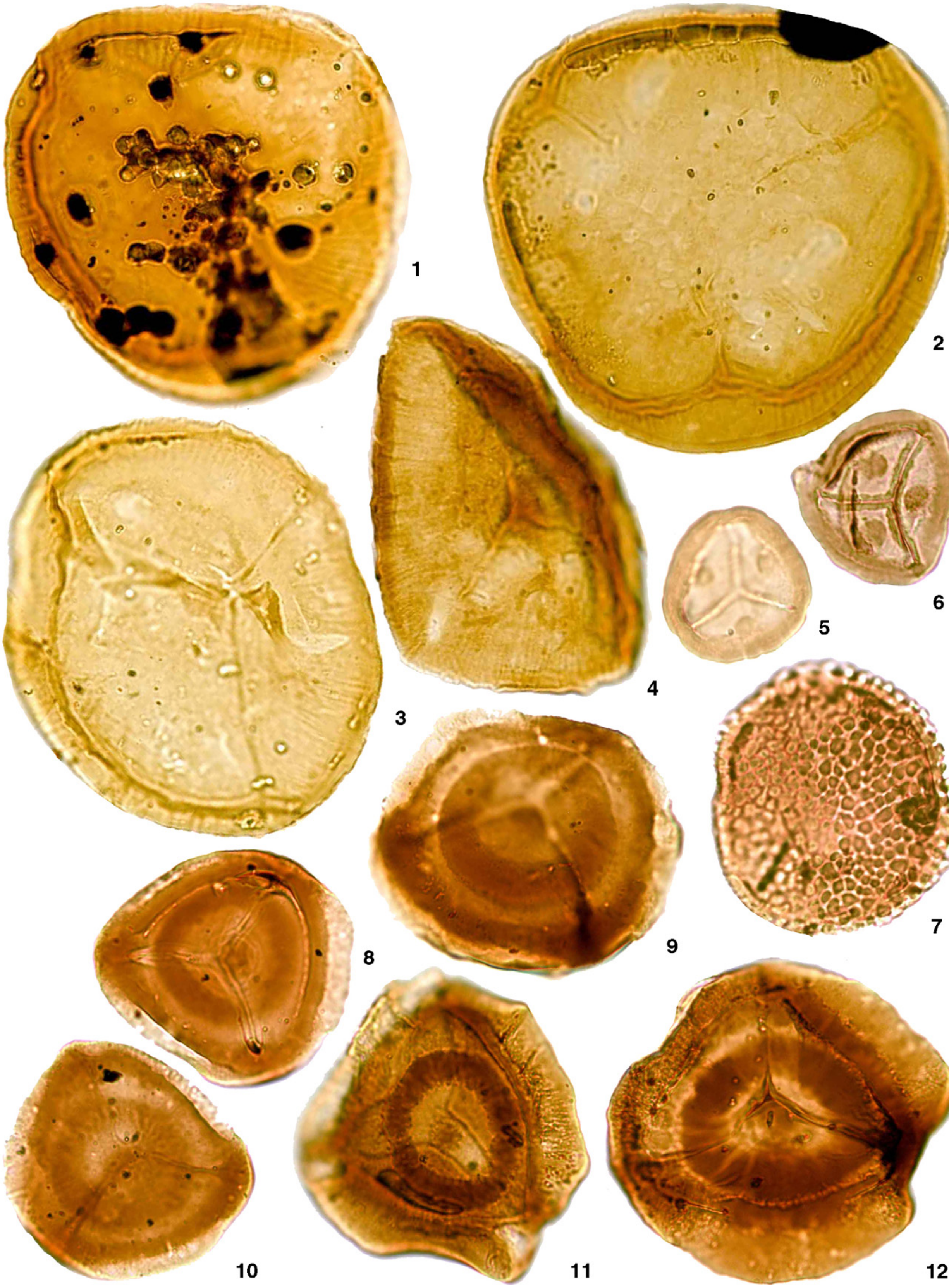

Plate 11.

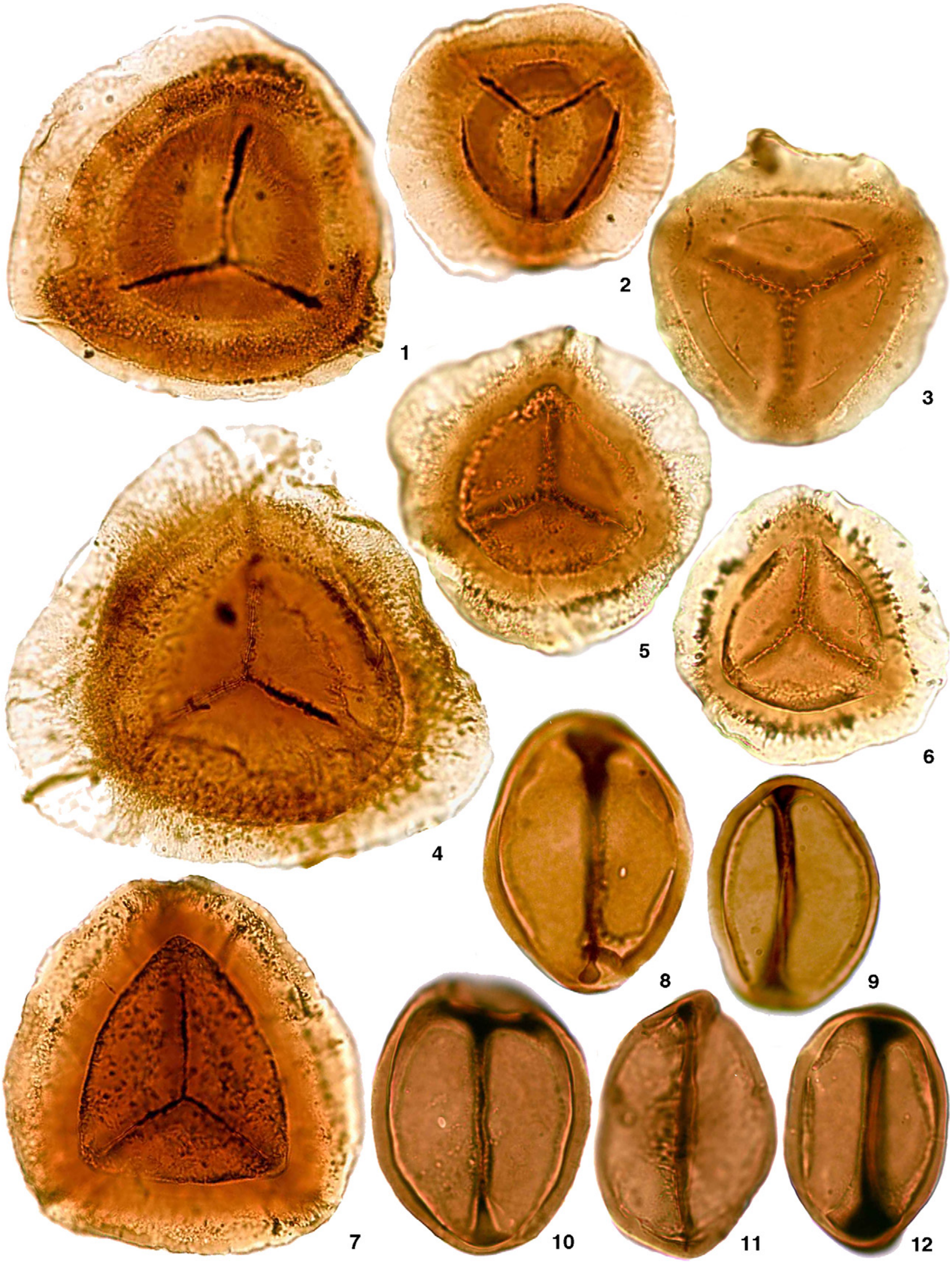

Plate 12.

Plate 10. **Fig. 1**. *Scylaspora costulosa* nov. sp. JNDL-3, 353.8', 03CW159, L33/3. **Fig. 2**. *Scylaspora costulosa* nov. sp. BAQA-1, 227.1', 03CW110, L24. Holotype. **Fig. 3**. *Scylaspora costulosa* nov. sp. BAQA-2, 50.8', 03CW127, O49/1. Paratype. **Fig. 4**. *Scylaspora costulosa* nov. sp. BAQA-2, 133.0', 03CW136, M45/1. **Fig. 5**. *Scylaspora costulosa* nov. sp. BAQA-2, 50.8', 03CW127, J40. **Fig. 6**. *Squamispora arabica* nov. gen. and sp. JNDL-1, 172.7', 60846, H29. Paratype. **Fig. 7**. *Squamispora arabica* nov. gen. and sp. JNDL-1, 177.0', PPM009, H45. **Fig. 8**. *Squamispora arabica* nov. gen. and sp. JNDL-1, 174.6', PPM008, C43. **Fig. 9**. *Squamispora arabica* nov. gen. and sp. JNDL-1, 174.6', 60848, L40/2. Paratype. **Fig. 10**. *Squamispora arabica* nov. gen. and sp. JNDL-1, 177.0', 60849, U31. Holotype.

Plate 11. **Fig. 1**. *Stellatispora multicostata* nov. sp. JNDL-3, 462.3', 03CW175, L30-31. **Fig. 2**. *Stellatispora multicostata* nov. sp. JNDL-4, 182.5', 03CW220, U41/4. Holotype. **Fig. 3**. *Stellatispora multicostata* nov. sp. JNDL-3, 462.3', 03CW175, H26. Paratype. **Fig. 4**. *Stellatispora multicostata* nov. sp. JNDL-4, 197.8', 03CW224, H39/3. **Fig. 5**. *Synorisporites papillensis* McGregor, 1973. BAQA-1, 376.4', 03CW119, C26/3. **Fig. 6**. *Synorisporites papillensis* McGregor, 1973. BAQA-1, 308.3', 03CW112, H40/4. **Fig. 7**. *Verrucosisporites polygonalis* Lanninger, 1968. BAQA-1, 406.0', 03CW123, M48/3. **Fig. 8**. *Zonotriletes armillatus* nov. sp. JNDL-1, 156.0', PPM004, P43. Holotype. **Fig. 9**. *Zonotriletes armillatus* nov. sp. JNDL-1, 156.0', 60840, X32/3. **Fig. 10**. *Zonotriletes armillatus* nov. sp. JNDL-1, 155.6', 60837, O34. **Fig. 11**. *Zonotriletes armillatus* nov. sp. JNDL-1, 155.6', PPM003, P30/4. **Fig. 12**. *Zonotriletes armillatus* nov. sp. JNDL-1, 155.6', 60838, J43/1.

Plate 12. **Fig. 1**. *Zonotriletes armillatus* nov. sp. JNDL-1, 162.3', 60841, F29/1. Paratype. **Fig. 2**. *Zonotriletes armillatus* nov. sp. JNDL-1, 167.8', 60843, L41. Paratype. **Fig. 3**. *Zonotriletes simplicissimus* nov. sp. JNDL-1, 177.0', PPM009, R47/1. **Fig. 4**. *Zonotriletes simplicissimus* nov. sp. JNDL-1, 172.7', 60845, F28/1. Paratype. The transverse attachment lines of the flange on the central body are distinguishable. **Fig. 5**. *Zonotriletes simplicissimus* nov. sp. JNDL-1, 177.0', PPM009, P32/4. Holotype. **Fig. 6**. *Zonotriletes simplicissimus* nov. sp. JNDL-1, 177.0', 60850, K44/2. The transverse attachment lines of the flange on the central body are distinguishable. **Fig. 7**. *Zonotriletes simplicissimus* nov. sp. JNDL-1, 177.0', 60849, K43/3. Paratype. **Fig. 8**. *Latosporites ovalis* nov. sp. BAQA-1, 222.5', 03CW108, F40. Paratype. **Fig. 9**. *Latosporites ovalis* nov. sp. BAQA-1, 345.5', 03CW114, K23. Holotype. **Fig. 10**. *Latosporites ovalis* nov. sp. BAQA-2, 54.8', 03CW129, Q36. **Fig. 11**. *Latosporites ovalis* nov. sp. BAQA-1, 371.1', 03CW118, R45. **Fig. 12**. *Latosporites ovalis* nov. sp. BAQA-2, 52.0', 03CW128, Q51/3.

Description: Amb circular to sub-circular. The hilum is well defined by a curvatura and its slightly granulate character is barely perceptible. Narrow, radial, irregular scars commonly characterize the proximal surface. The hilum radius equals about 3/4 of the amb radius. Exospore is sculptured subequatorially and distally with evenly distributed and spaced elements 0.5-1.5 μm high and 1–3 μm apart. The ornamentation varies from bacula to spinae and coni. Exospore 1–3 μm thick.

Dimensions: 48 (58) 70 μm, 28 specimens measured.

Comparison: *Cymbohilates amplus* Wellman and Richardson, 1996 possesses a very similar distal ornamentation but it is significantly larger (73–104 μm) than *Cymbohilates comptulus* nov. sp. Moreover, *Cymbohilates amplus* does not possess narrow radial tears in the exospore on the proximal surface. *Gneudnaspora* sp. in Balme (1988) also appears very similar to *Cymbohilates comptulus* nov. sp., however it is only represented by a single specimen that is ornamented with evenly disposed cones about 1 μm high and 1 μm in basal diameter.

Occurrence: Boreholes BAQA-1, 2 and JNDL-4. Jauf Formation (Sha'iba-Hammamiyat members). Pragian-Emsian.

Cymbohilates heteroverrucosus nov. sp.

Plate 2, Figs. 9–12; Plate 3, Figs. 1 and 2

Derivation of name: Refers to the ornament variability on a same specimen; *hetero-* = different, *verrucosus* = bearing verrucae (Latin).

Holotype: Plate 2, Fig. 10, borehole JNDL-1, sample 167.8', slide 60843, EFC D27/3.

Paratype: Plate 3, Fig. 2, borehole JNDL-1, sample 177.0', slide 60849, EFC H44.

Diagnosis: A *Cymbohilates* bearing verrucae and bacula of different type and size, which are distributed unevenly on the whole surface of the cryptospore.

Description: Amb circular to sub-circular. Hilum often is barely perceptible and commonly shows narrow scars that may resemble a pseudo-trilete mark. Distal and proximal surfaces bear a varied sculpture of verrucae and bacula, 0.5–7 μm wide at base and up to 4 μm high. The elements can have a flared base or more parallel sides. The ornament size and type can be very variable on the same specimen. The small and largest elements are distributed unevenly, however the contact area normally possesses the smallest verrucae.

Dimensions: 45 (53) 62 μm, 34 specimens measured.

Occurrence: Boreholes JNDL-1, 3, 4. Jauf (Hammamiyat-Murayr members) and Jubah formations. Emsian-Givetian.

Genus ***Gneudnaspora*** Balme, 1988 emend.

1991. *Laevolancis* – Burgess and Richardson, p. 606.

Type species: *Gneudnaspora kernickii* Balme, 1988.

Emended diagnosis: Proximally hilate cryptospore monads. Amb circular to oval. Exospore alveolate or laevigate, proximally attenuated. Contact face bordered by a weakly to strongly developed circular to oval curvatural ridge. Different types of scars can be present on the contact face, from an irregular, simple, pseudo-trilete or pseudo-tetralete scar to an irregular sub-stellate opening.

Remark: The material in the present study is very similar to that figured and described by Balme (1988) and the authors consider that the proximal structure of *Gneudnaspora* has been misinterpreted by Balme. It corresponds to scars, sometimes looking like a trilete or monolete mark, but commonly having no particular shape. In addition, some specimens do not show these scars and are therefore similar to genus *Laevolancis* Burgess and Richardson, 1991 described from the Silurian. Finally, we consider that the latter form is a junior synonym of the genus *Gneudnaspora* Balme, 1988, following the diagnosis as emended here.

The diagnosis of the genus *Gneudnaspora* is restricted to include only proximally hilate cryptospore monads that are entirely laevigate. Thus, *Gneudnaspora* sp. in Balme (1988), which bears small cones, has to be allocated to the genus *Cymbohilates* Richardson, 1996 emended here. As *Gneudnaspora* *divellomedia* (Chibrikova) Balme, 1988 is here considered to be the valid combination, the type species for *Laevolancis*, *L. divellomedia* (Chibrikova) Burgess and Richardson, 1991, becomes invalid. The existing species of *Laevolancis* are herein transferred to *Gneudnaspora*.

Gneudnaspora divellomedia (Chibrikova) Balme, 1988 var. *divellomedia*

Plate 3, Figs. 3–9

1988. *Gneudnaspora divellomedium* (Chibrikova) – Balme, p. 125, Plate 3, Figs. 1–7.

Diagnosis: An entirely laevigate *Gneudnaspora* showing different types of scars on its contact face.

Description: Amb circular to sub-circular. A diffuse to clear curvatura delimits a more or less circular hilum. The hilum radius equals 3/4 to 6/7 amb radius. Contact face shows different types of scars, from an irregular, simple, pseudo-trilete or pseudo-tetralete, to an irregular sub-stellate shape. Proximal and distal surfaces are entirely laevigate.

Dimensions: 32 (54) 82 μm, 17 specimens measured.

Remark and comparison: Specimens assigned to *Laevolancis divellomedia* (Chibrikova) Burgess and Richardson, 1991 are not considered here to be conspecific with *Gneudnaspora divellomedia* (Chibrikova) Balme, 1988 var. *divellomedia*. *Laevolancis divellomedia* is generally smaller than *Gneudnaspora divellomedia* var. *divellomedia*. Furthermore, the former species very often shows an intact contact face whilst the latter usually possesses different types of scars.

Occurrence: Boreholes BAQA-1, 2 and JNDL-1, 3, 4. Jauf (upper Sha'iba-Murayr members) and Jubah formations. Emsian-Givetian.

Gneudnaspora divellomedia (Chibrikova) Balme, 1988 var. *minor* nov. var.

Plate 3, Figs. 10–16

1959. *Archaeozonotriletes divellomedium* – Chibrikova p. 65, Plate 9, Fig. 4.

1966b. *Hispanaediscus bernesgae* – Cramer p. 82, Plate 1, Figs. 2 and 11, Text-fig. 2.

1968. Spore no. 2651 – Magloire, 1968, Plate 1, Fig. 6.

1969.?*Archaeozonotriletes* cf. *divellomedium* Chibrikova – Richardson and Lister, p. 238, Plate 43, Fig. 12.

1974. *Archaeozonotriletes* (?) *divellomedium* (Chibrikova) – Arkhangelskaya Plate 1, Fig. 51.

1974. *Zonaletes* (?) *divellomedium* (Chibrikova) – Arkhangelskaya, Plate 6, Figs. 3 and 4.

1974.?*Archaeozonotriletes divellomedium* Chibrikova – McGregor Plate 1, Figs. 35 and 40.

1978. *Hispanaediscus* sp. – McGregor and Narbonne, 1978, p. 1296, Plate 1, Figs. 20–22.

1980. *Zonaletes* (?) *divellomedium* (Chibrikova) – Arkhangelskaya Plate 5, Fig. 34.

1984.?*Stenozonotriletes irregularis* (Schultz) – McGregor p. 37, Plate 1, Fig. 26.

1986. *Archaeozonotriletes* cf. *divellomedium* Chibrikova – Buret and Moreau-Benoît, 1986, Plate 1, Fig. 1.

1986. *Tholisporites divellomedium* (Chibrikova) – Turnau, p. 349, Plate 2, Fig. 12, Plate 4, Fig. 14.

1991. *Laevolancis divellomedia* (Chibrikova) – Burgess and Richardson, p. 607, Plate 2, Figs. 4 and 6.

Derivation of name: Refers to the small size of the amb; *minor* = smaller (Latin).

Holotype: Plate 3, Fig. 15, borehole BAQA-2, sample 50.2', slide 03CW126, EFC B49/2.

Paratype: Plate 3, Fig. 12, borehole BAQA-2, sample 54.8', slide 03CW129, EFC G49.

Diagnosis: A *Gneudnaspora* of small size, very simple form.

Description: Amb circular to sub-circular. A diffuse to clear curvatura delimits a more or less circular hilum. Hilum radius is commonly 3/4 to 4/5 spore radius. Contact face sometimes shows a small simple scar. Proximal and distal surfaces are entirely laevigate.

Dimensions: 28 (31) 34 μm, 21 specimens measured.

Remark: As the genus *Laevolancis* Burgess and Richardson, 1991 is here considered to be a junior synonym of genus *Gneudnaspora* Balme, 1988, *Laevolancis divellomedia* (Chibrikova) Burgess and Richardson, 1991 requires reassignment. Since it is suggested above that *Laevolancis divellomedia* differs from *Gneudnaspora divellomedia* (Chibrikova) Balme, 1988 var. *divellomedia*, the reassignment necessitates introduction of a new variety, *Gneudnaspora divellomedia* (Chibrikova) Balme, 1988 var. *minor* nov. var.

Comparison: *Gneudnaspora divellomedia* (Chibrikova) Balme, 1988 var. *divellomedia* has a similar structure but is larger (32–82 μm). The smaller new variety shows a little size variability. Furthermore, the larger variety always possesses different types of scars, unlike *Gneudnaspora divellomedia* (Chibrikova) Balme, 1988 var. *minor* nov. var., which often possesses an intact contact face. *Gneudnaspora plicata* (Burgess and Richardson) nov. comb. appears very similar and is thus difficult to distinguish, however it is only known from Wenlock strata. Steemans et al. (1996) define a morphon which includes the two taxa and record intermediate forms with a range of thin to thick wall thicknesses.

Occurrence: Boreholes BAQA-1, 2 and JNDL-1, 3, 4. Jauf (Sha'iba-Murayr members) and Jubah formations. Pragian-Givetian.

Gneudnaspora plicata (Burgess and Richardson) nov. comb.

1991. *Gneudnaspora plicata* – Burgess and Richardson, p. 607, Plate 2, Fig. 8.

Remark: As the genus *Laevolancis* Burgess and Richardson, 1991 is here considered to be a junior synonym of genus *Gneudnaspora* Balme, 1988, other species that have been described under *Laevolancis* become invalid and have to be transferred to the valid genus. *Gneudnaspora plicata* (Burgess and Richardson) nov. comb. is not recorded in the present assemblages.

Gneudnaspora chibrikovae (Steemans et al.) nov. comb.

2000. *Gneudnaspora chibrikovae* – Steemans et al. p. 99, Plate 2, Figs. n–o; Plate 3, Fig. a.

Remark: *Gneudnaspora chibrikovae* (Steemans et al.) nov. comb. does not occur in the present assemblages.

5.2.2. Trilete spores

Genus ***Camarozonotriletes*** Naumova ex Ishchenko, 1952

Type species: *Camarozonotriletes devonicus* Naumova, 1953.

Camarozonotriletes filatoffii nov. sp.

Plate 4, Figs. 14–23; Plate 5, Fig. 1

?1972.?*Reticulatisporites* sp. – Kemp, p. 115, Plate 55, Fig. 9.

Derivation of name: After the name of the Australian palynologist employed by Saudi Aramco, John Filatoff.

Holotype: Plate 4, Fig. 22, borehole BAQA-2, sample 133.0', slide 03CW136, H25.

Paratypes: Plate 4, Fig. 19, borehole BAQA-1, sample 222.5', slide 03CW108, W30. Plate 4, Fig. 21, borehole BAQA-1, sample 223.5', slide 03CW109, EFC M37.

Diagnosis: A small *Camarozonotriletes* with an indistinctly defined spine-bearing reticulum.

Description: Amb sub-circular to sub-triangular. Contact area sub-triangular to triangular with rounded corners and laevigate. Laesurae simple or accompanied by narrow labra, straight, 3/5 to 4/5 of the radius in length. Exospore darker adjacent to rays, forming a more or less triangular darkened and presumably thickened zone around the proximal pole and extending to the end of the rays. Cingulum 1–2 μm thick equatorially opposite the trilete rays and up to 6 μm interradially. Distal and equatorial sculpture composed of spines generally 1–2 μm high, 0.5–1.5 μm wide at their base, and 1.5–2.5 apart. Elements are commonly situated on indistinctly defined muri, about 1–2.5 μm wide, that form a reticulum. Lumina are generally 3–7 μm in their longest diameter. Cingulum slightly darker than central area.

Dimensions: 24 (29) 35 μm, 35 specimens measured.

Comparison: The distal sculpture distinguishes *Camarozonotriletes filatoffii* nov. sp. from all other species of *Camarozonotriletes*. *Camarozonotriletes sextantii* McGregor and Camfield, 1976 is larger (37–60 μm). Its distal and equatorial sculpture does not possess a reticulum and the ornaments are evenly distributed.?*Reticulatisporites* sp. in Kemp (1972) is similar but does not exhibit spines on the reticulum.

Occurrence: Boreholes BAQA-1, 2 and JNDL-3, 4. Jauf Formation (Sha'iba-Murayr members). Pragian-Emsian.

Camarozonotriletes rugulosus nov. sp.

Plate 5, Figs. 2–9

Derivation of name: Refers to the wrinkled appearance of the distal face; *rugulosus* = slightly wrinkled (Latin).

Holotype: Plate 5, Fig. 2, borehole JNDL-1, sample 156.0', slide 60840, EFC T48.

Paratypes: Plate 5, Fig. 4, borehole JNDL-1, sample and slide 156.0', slide 60839, EFC M49/3. Plate 5, Fig. 6, borehole JNDL-1, sample 172.7', slide 60846, EFC P46/2.

Diagnosis: A triangular *Camarozonotriletes* with thin rugulae.

Description: Amb triangular. The corners are slightly rounded, while the margins are slightly convex, straight, or sometimes slightly concave. Exospore thin. Laesurae distinct, simple and straight. The trilete mark radius is at least longer than 4/5 of the amb radius. Curvaturae are not easily distinguishable. Cingulum generally 1–2 μm thick equatorially opposite the trilete rays and 3–5 μm interradially. Contact faces laevigate. Distal face sculptured with very thin, 0.5 μm in maximum width.

Dimensions: 37 (46) 59 μm, 30 specimens measured.

Comparison: *Leiotriletes horridulus* Ishchenko, 1958, an Upper Mississippian species of Russia, resembles *Camarozonotriletes rugulosus* nov. sp. according to the original description, but it is smaller (30–35 μm). Furthermore, this taxon is not interradially thickened.

Remark: As the rugulae are very thin, they may be barely visible or undistinguishable because of bad preservation. Its thin exospore seems delicate.

Occurrence: Borehole JNDL-1. Jubah Formation. Givetian.

Genus ***Cymbosporites*** Allen, 1965

Type species: *Cymbosporites cyathus* Allen, 1965.

Cymbosporites asymmetricus nov. sp.

Plate 5, Figs. 15–19; Plate 6, Figs. 1 and 2

Derivation of name: Refers to the asymmetry of the trilete mark; *asymmetricus* = asymmetrical (Latin).

Holotype: Plate 6, Fig. 1, borehole JNDL-3, sample 413.2', slide 03CW166, EFC T42/1.

Paratype: Plate 5, Fig. 16, borehole JNDL-4, sample 160.7', slide 03CW211, EFC V42.

Diagnosis: A *Cymbosporites* with small spines densely distributed. One interradial area of the contact surface is smaller than the other two.

Description: Amb oval to sub-triangular with a distinctly elongate axis aligned with one of the laesurae. Contact faces laevigate with the one, transected by the long axis, being smaller than its neighbours. The smallest interradial angle, formed by the two shorter trilete mark branches, is commonly between 70° and 100°. Laesurae distinct, straight to slightly sinuous and accompanied by prominent labra commonly 1–2.5 μm in overall width. Radius of contact surface generally equals to 3/4 of the amb radius. Proximo-equatorial and distal regions patinate and sculptured with spines (ca. 1 μm high), which are densely distributed. Some specimens can exhibit slight separations of the exospore. Exospore 2–4 μm thick.

Dimensions: 36 (51) 67 μm, 15 specimens measured.

Comparison: *Apiculiretusispora plicata* (Allen) Streel, 1967, has a similar size and ornamentation, and sometimes also an asymmetrically placed laesurae, but differs in not being patinate.

Occurrence: Boreholes JNDL-3, 4. Jauf Formation (Subbat-Murayr members). Emsian.

Genus ***Dibolisporites*** Richardson, 1965

Type species: *Dibolisporites echinaceus* (Eisenack) Richardson, 1965.

Dibolisporites pilatus nov. sp.
Plate 6, Figs. 10–13

Derivation of name: Refers to the pilate distal surface; *pilatus* = made up of pila (Latin).

Holotype: Plate 6, Fig. 11, borehole JNDL-1, sample 167.8', slide PPM006, EFC V48.

Paratype: Plate 6, Fig. 13, borehole JNDL-1, sample 167.8', slide 60842, EFC R42/3.

Diagnosis: A thick-walled *Dibolisporites* with high pilate elements irregularly distributed.

Description: Amb sub-triangular to sub-circular. Exospore 3–6.5 μm thick equatorially. Contact faces laevigate. Laesurae distinct, straight to slightly sinuous and accompanied by labra up to 4 μm in overall width. Distal surface sculptured with pila or other constricted ornaments with parallel sides, which always possess a rounded top. The elements are commonly 2–4 μm wide at base and 4–7 μm high, rarely 10 μm high. The ornament size is very variable on the same specimen; short and tall elements are irregularly distributed.

Dimensions: 54 (68) 79 μm, 27 specimens measured.

Remark: This taxon cannot be attributed to the genus *Raistrickia* Schopf et al., 1944 emend. Potonié and Kremp, 1954 because this latter includes forms sculptured with rather abruptly blunted elements.

Occurrence: Borehole JNDL-1. Jubah Formation. Givetian.

Genus ***Dictyotriletes*** (Naumova) Potonié and Kremp, 1954

Type species: *Dyctyotriletes mediareticulatus* (Ibrahim) Potonié and Kremp, 1954.

Dictyotriletes biornatus nov. sp.
Plate 7, Figs. 1–9

Derivation of name: Refers to the muri formed by rows of grana; *biornatus* = two ornament types (Latin).

Holotype: Plate 7, Fig. 5, borehole BAQA-1, sample 345.5', slide 03CW114, EFC O53.

Paratypes: Plate 7, Fig. 3, borehole BAQA-1, sample 366.9', slide 03CW117, EFC L27/1. Plate 7, Fig. 8, borehole BAQA-1, sample 219.2', slide 03CW107, EFC L40/4.

Diagnosis: A *Dictyotriletes* with muri formed by grana.

Description: Amb triangular to sub-circular. Trilete mark rarely visible. Exospore thin proximally. Distal and proximo-equatorial areas are thicker and reticulate. Muri of reticulum formed by orientated rows of grana (1–2 μm wide) that are commonly merged at the base. Polygonal lumina of reticulum 4–9 μm in greatest diameter is about 30 to 40 in number.

Dimensions: 41 (55) 71 μm, 29 specimens measured.

Remark: Some specimens show a further merging of several grana so as to form solid muri. Other specimens, which are not attributed to *Dictyotriletes biornatus* nov. sp., have less well organized lumina with some grana occurring inside the lumina. All these specimens are probably related and need further investigation.

Occurrence: Boreholes BAQA-1, 2 and JNDL-3. Jauf Formation (upper Sha'iba-Hammamiyat members). Emsian.

Genus ***Scylaspora*** Burgess and Richardson, 1995

Type species: *Scylaspora scripta* Burgess and Richardson, 1995.

Scylaspora costulosa nov. sp.
Plate 10, Figs. 1–5

Derivation of name: Refers to the nature of the contact faces, *costulosus* = possessing weakly defined ribs (Latin).

Holotype: Plate 10, Fig. 2, borehole BAQA-1, sample 227.1', slide 03CW110, EFC L24.

Paratype: Plate 10, Fig. 3, borehole BAQA-2, sample 50.8', slide 03CW127, EFC O49/1.

Diagnosis: A *Scylaspora* with anastomosing sinuous muri or rugulae on the contact faces. Muri are more perceptible towards the curvaturae.

Description: Amb circular to sub-circular. Distal surface strongly convex. Proximal surface flattened pyramidal with weakly concave contact faces that are delimited equatorially by curvaturae perfectae. Trilete mark often gaping at the proximal pole. Laesurae distinct, simple and straight. There is marked encroachment of the distal surface due to invagination of adjacent curvaturae where they conjoin at the radial extremities. The muri on contact faces (ca. 1 μm wide) are generally radially aligned but are slightly sinuous and rugulate in places. They are obvious close to the curvaturae perfectae and commonly become faint towards the proximal pole. Exospore outside the contact faces entirely laevigate, and 1–2.5 μm thick equatorially.

Dimensions: 46 (65) 90 μm, 14 specimens measured.

Comparison: *Scylaspora rugulata* (Riegel) nov. comb. has a darker subtriangular area at the proximal pole and the muri are more prominent, more angular and visible on the whole contact surface. *Scylaspora chartulata* (McGregor and Narbonne, 1978) Rubinstein and Steemans, 2002 appears very similar but may possess minute, closely spaced grana on the contact areas. *Scylaspora fayersii* Wellman, 2007 possesses very similar muri but also a subtriangular-subcircular area of thinner exospore centered on the proximal pole that extends 1/3 to 1/2 of the way to the equator. This area is surrounded by a discrete dark band of thickened exospore. Moreover, this species is smaller (33–50 μm) than *Scylaspora costulosa* nov. sp.

Occurrence: Boreholes BAQA-1, 2 and JNDL-3, 4. Jauf Formation (Sha'iba-Murayr members). Pragian-Emsian.

Scylaspora rugulata (Riegel) nov. comb.

1965. *Retusotriletes dubius* (Eisenack) – Richardson, p. 564, Plate 88, Fig. 6.

1973. *Retusotriletes rugulatus* – Riegel, p. 82, Plate 10, Figs. 2–5.

Remark: *Retusotriletes rugulatus* Riegel, 1973 is not recorded in the present assemblages but is here reassigned to the genus *Scylaspora* Burgess and Richardson, 1995 because it possesses the typical proximal sculpture of this genus. As Rubinstein and Steemans (2002) consider the genus *Rugosisporites* Dufka ex Jansonius et al., 1998 to be a junior synonym of *Scylaspora*, its type species is reassigned here to the valid genus.

Scylaspora kozlicus (Dufka ex Jansonius et al.) nov. comb.
1995. *Scylaspora kozlicus* – Dufka p. 72, Plate 2, Figs. 15 and 17.

Remark: This taxon does not occur in the assemblages studied here.

Genus ***Squamispora*** nov. gen.

Derivation of name: Refers to the scaly appearance of the distal face; *squameus* = scaly, flaky (Latin).

Type species: *Squamispora arabica* nov. sp.

Diagnosis: Trilete miospores with a two-layered exospore. The entire surface of the spore is covered by flakes, which are derived from the original outer layer. This discontinuous sculpture of exospore gives a scaly appearance. The two layers are not normally separated but local detachments can occur.

Comparison: *Tholisporites ancylus* Allen, 1965 also has an outer layer. The author regards this 'sculpturing' as the result of corrosion of a punctate exospore rather than being a true sculptural pattern.

Remark: No genera exist in the literature to accommodate such forms. They cannot even be compared to genera such *Verrucosisporites* Ibrahim, 1933 because the flakes do not constitute normal ornaments.

Squamispora arabica nov. gen. and sp.
Plate 10, Figs. 6–10

Derivation of name: Refers to the locality where this species was found; *arabicus* = from Arabia (Latin).

Holotype: Plate 10, Fig. 10, borehole JNDL-1, sample 177.0', slide 60849, EFC U31.

Paratypes: Plate 10, Fig. 6, borehole JNDL-1, sample 172.7', slide 60846, EFC H29. Plate 10, Fig. 9, borehole JNDL-1, sample 174.6', slide 60848, EFC L40/2.

Diagnosis: A *Squamispora* with outer exosporal flakes of variable size and shape over the entire surface, forming an irregular mosaic.

Description: Amb sub-circular to sub-triangular. Exospore 1.5–4 μm thick equatorially. Laesurae distinct, simple and straight extending from the proximal pole for a half to all of the way to the equator. No curvaturae visible. The whole surface of the miospore is covered by closely spaced flakes. They are commonly 0.5–15 μm in maximum length, size and shape being quite variable within the taxon and also on a single specimen. Large and small flakes do not constitute an ordered pattern but resembles an irregular mosaic. Except for the flakes, exospore is entirely laevigate.

Dimensions: 39 (51) 63 μm, 43 specimens measured.

Remark: Squamispora arabica nov. gen. and sp. sometimes occurs in our material in clusters of several specimens.

Occurrence: Borehole JNDL-1. Jubah Formation. Givetian.

Genus ***Stellatispora*** Burgess and Richardson, 1995

Type species: *Stellatispora inframurinata* (Richardson and Lister, 1969) Burgess and Richardson, 1995.

Stellatispora multicostata nov. sp.
Plate 11, Figs. 1–4

Derivation of name: Refers to the costae; *multi-* = numerous, *costatus* = possessing costae (Latin).

Holotype: Plate 11, Fig. 2, borehole JNDL-4, sample 182.5', slide 03CW220, EFC U41/4.

Paratype: Plate 11, Fig. 3, borehole JNDL-3, sample 462.3', slide 03CW175, EFC H26.

Diagnosis: A large *Stellatispora* with many thin radial costae situated on the patina. Costae start at the curvaturae and gradually disappear towards the distal pole.

Description: Amb sub-circular to sub-triangular. Contact surfaces are thin and smooth and can be sometimes collapsed or absent. When present, laesurae are simple and straight. Outside the contact surfaces the exospore is two-layered and thicker, 2–6 μm thick at the equator. Patina is ornamented with many straight radial costae, 0.5–1 μm wide and 6–17 μm long, which start proximo-equatorially from the curvaturae and disappear towards the distal pole. From the amb, their length corresponds to 1/5 to 1/2 of the amb radius. The number of costae varies between 25 and 45 on each interradial area, and are weak to absent opposite the trilete rays.

Dimensions: 54 (73) 86 μm, 14 specimens measured.

Comparison: *Stellatispora inframurinata* var. *inframurinata* (Richardson and Lister, 1969) Burgess and Richardson, 1995 is smaller (30–49 μm) and displays a patina ornamented with radial elongated elements but these are thicker (1–3.5 μm wide), can bifurcate 2–3 times, and are occasionally convolute and discontinuous. *Tholisporites salantaicus* (Arkhangelskaya) Turnau, 1986 seems conspecific with *Stellatisporites multicostata* nov. sp. but shows radial costae on the contact faces as well as on the distal side.

Occurrence: Boreholes JNDL-3, 4. Jauf Formation (Subbat-Hammamiyat members). Emsian.

Genus ***Zonotriletes*** Luber and Waltz, 1938

Type species: None designated.

Zonotriletes armillatus nov. sp.
Plate 11, Figs. 9–12; Plate 12, Figs. 1 and 2

Derivation of name: Refers to the annulus situated on the distal face; *armillatus* = provided with an annulus (Latin).

Holotype: Plate 11, Fig. 8, borehole JNDL-1, sample 156.0', slide PPM004, EFC P43.

Paratypes: Plate 12, Fig. 1, borehole JNDL-1, sample 162.3', slide 60841, EFC F29/1. Plate 12, Fig. 2, borehole JNDL-1, sample 167.8', slide 60843, EFC L41.

Diagnosis: A *Zonotriletes* with a distal annulus. Flange is proximo-equatorial.

Description: Amb sub-circular to sub-triangular with convex sides and rounded corners. Laesurae distinct, straight to slightly sinuous, and accompanied by prominent labra, each up to 3 μm wide, extending to the inner margin of the zona. Curvaturae not visible. The central body radius equals 1/3 to 4/5 amb radius. Exospore of the central body is commonly 2–4 μm thick equatorially, rarely up to 6 μm. The thin proximo-equatorial flange is generally 4–10 μm wide interradially but sometimes up to about 20 μm for the larger specimens. The flange is always narrower opposite the trilete rays. It sometimes is radially folded and can be folded back over the central body locally. Thin transverse attachment lines of the flange on the central body often can be distinguished on the proximal face. An annulus is present on the distal face and is 4–10 μm wide. The annulus radius equals 5/10 to 7/10 central body radius. The annulus is often homogeneous, darker than the distal exospore and striped in some cases. A small circular dark area inside the annulus occurs at the distal pole. Proximal and distal surfaces laevigate.

Dimensions: 43 (64) 109 μm, 35 specimens measured.

Comparison: *Breconisporites breconensis* Richardson et al., 1982 has a larger distal annulus which can be partially or completely coincident with the cingulum giving the appearance of a broad thickened zone. Moreover, the transverse attachment lines of the flange on the proximal face form plicate ridges up to 1.5 μm wide. Furthermore, the flange is commonly narrower in the radial zones. *Zonotriletes armillatus* nov. sp. can be confused with *Zonotriletes simplicissimus* nov. sp. when the specimens are poorly preserved and dark colored, making the distal annulus difficult to discern.

Occurrence: Borehole JNDL-1. Jubah Formation. Givetian.

Zonotriletes simplicissimus nov. sp.

Plate 12, Figs. 3–7

?1968. *Zonotriletes* sp. 3 – Jardiné and Yapaudjian, p. 461, Plate 2, Fig. 2.

Derivation of name: Refers to the simplicity of the structure; *simplicissimus* = very simple (Latin).

Holotype: Plate 12, Fig. 5, borehole JNDL-1, sample 177.0’, slide PPM009, EFC P32/4.

Paratypes: Plate 12, Fig. 4, borehole JNDL-1, sample 172.7’, slide 60845, EFC F28/1. Plate 12, Fig. 7, borehole JNDL-1, sample 177.0’, slide 60849, EFC K43/3.

Diagnosis: A laevigate *Zonotriletes* with thick laesurae and equatorially thick central body. Flange is proximo-equatorial.

Description: Amb sub-triangular with convex sides and rounded corners. Laesurae distinct, straight to slightly sinuous, 3–7 μm in overall width, extending to the inner margin of the zona. Curvaturae not visible. Central body radius equals 3/5 to 4/5 amb radius. Exospore of the central body is 3–7 μm thick equatorially. The thin proximo-equatorial flange is commonly 4–13 μm wide interradially but sometimes larger, up to 18 μm. The flange is generally narrower opposite the trilete rays and is sometimes radially folded. Thin transverse attachment lines of the flange on the central body often can be distinguished. Proximal and distal surfaces entirely laevigate.

Dimensions: 38 (59) 82 μm, 26 specimens measured.

Comparison: *Perotrilites caperatus* (McGregor) Steemans, 1989 possesses a coarse wrinkled exospore over the equatorial part of the proximal face and is distally verrucate or rugulate. *Cingulizonates glaber* Arkhangelskaya, 1978 seems morphologically close but it has a fairly large, rounded area of very thin, sometimes ruptured, wall at the proximal pole, 22–35 μm in diameter, and its laesurae are simple and slender. *Breconisporites simplex* Wellman, 1993 seems also similar, but it possesses narrower laesurae and folded contact areas. *Zonotriletes* sp. 3 in Jardiné and Yapaudjian (1968) appears similar to *Zonotriletes simplicissimus* nov. sp. according to the figure, but there is no description to allow a detailed comparison.

Remark: The smallest specimens commonly have a less well-developed proximo-equatorial flange when compared to the largest ones which can possess a very wide flange interradially.

Occurrence: Borehole JNDL-1. Jubah Formation. Givetian.

5.2.3. Monolete spores

Genus ***Latosporites*** Potonié and Kremp, 1954

Type species: *Latosporites latus* Potonié and Kremp, 1954.

Latosporites ovalis nov. sp.

Plate 12, Figs. 8–12

?1965. *Laevigatosporites antiqus* – Moreau-Benoit, p. 231, Plate 3, Figs. 54 and 55.

?2007. ?monolete spore – Wellman, Plate 19, Fig. h.

Derivation of name: Refers to the shape of the amb; *ovalis* = oval (Latin).

Holotype: Plate 12, Fig. 9, borehole BAQA-1, slide sample 345.5’, slide 03CW114, EFC K23.

Paratype: Plate 12, Fig. 8, borehole BAQA-1, slide sample 222.5’, slide 03CW108, EFC F40.

Diagnosis: A laevigate *Latosporites* with suture extending almost to equator and accompanied by distinctive labra.

Description: Amb elliptical to oval. The length of the short axis generally equals to 7/10 of the long axis. Suture distinct, straight to slightly curved and accompanied by distinctive labra 2–5 μm in overall width. Suture extending almost to equator and terminating in well defined curvaturae. Exospore entirely laevigate, 1.5–3 μm thick.

Dimensions: 32 (48) 62 μm, 22 specimens measured.

Comparison: *Latosporites* sp. A and *Latosporites* sp. B in Owens (1971) are larger and have a thicker exospore. *Latosporites* sp. B has a finely granulate exospore and lacks prominent labra. Latosporites sp. in McGregor (1960) possesses a short, poorly defined Y-like bifurcation. *Limbomonoletes lenis* Arkhangelskaya, 1985 has a thinner exospore and is cingulate. *Devonomonoletes* Arkhangelskaya, 1985 is ornamented outside the contact surface. *Laevigatosporites antiqus* Moreau-Benoît, 1965 possibly represents the same taxon but the description is too succinct for detailed comparison. *Laevigatosporites* sp. in McGregor and Camfield (1982) is more elongate. Its suture is simple and extends about 1/2 to 5/6 of the longest diameter of spore. *Laevigatosporites* sp. in de Jersey (1966) is small and its sutura extends about half-length of spore and the exospore can be very faintly scabrate. Wellman (2007) has probably found a similar monolete spore in the Rhynie Outlier in Scotland.

Occurrence: Boreholes BAQA-1, 2 and JNDL-3, 4.

6. Description of the palynological assemblages

Diverse assemblages of well-preserved palynomorphs were recovered from throughout the investigated sequence (Fig. 2;

Appendix A). Most contain a mixture of terrestrial (spores, phytodebris and in some cases possible aquatic algae) and marine elements (acritarchs, prasinophycean algal cysts, occasionally scolecodonts and very rarely chitinozoans). Most of the assemblages are dominated by spores and phytodebris, with marine elements generally rather rare. Some assemblages in the Hammamiyat and Murayr members are dominated by sphaeromorphs, often associated with acritarchs. The significance of these highly characteristic assemblages is discussed below. A single sample/horizon from the Hammamiyat Member in JNDL-4 is notable because of the abundance of chitinozoans, that elsewhere are absent. Appendix A lists all of the taxa encountered and their observed distribution in the samples. The assemblages are interpreted as reflecting nearshore, shallow marine depositional conditions, characterized by a very high terrestrial input, and variable marine influence.

Most assemblages are dominated by a diversity of well-preserved spores, and these are of most use in biostratigraphical dating and correlation of the deposits. A quantitative study of spore diversity and abundances is currently being undertaken by one of us (PB), so we will only provide a brief (non-quantitative) review of the characteristics of the spore assemblages in the biostratigraphical analysis that follows. The stratigraphy of typical species from Euramerican zonations is discussed firstly in Breuer et al. (2005) and below here. In addition, the ranges of new species described here are taken into account.

The oldest spore assemblages are those from the Sha'iba Member (Jauf Formation) in BAQA-1 (Fig. 2; Appendix A). They are dominated by trilete spores with subsidiary cryptospores (predominantly hilate cryptospores). The most common trilete spore morphotype is retusoid. Laevigate retusoid trilete spores are fairly abundant (mainly assigned to *Retusotriletes* spp., but also including *R. maculatus* and the intriguing taxon *Scylaspora costulosa* sp. nov.). The vast majority of retusoid trilete spores have apiculate ornament and belong to the genus *Apiculiretusispora*. At least three species of *Apiculiretusispora* are present, including specimens that are clearly bilayered with the characteristic sloughing exospore. Other apiculate retusoid trilete spores belong to the genus *Dibolisporites* that is relatively abundant. At least two species of *Dibolisporites* can be recognized, and they exhibit a wide diversity of ornament types, including various shapes of biform elements. More highly ornamented retusoid trilete spores are represented by the genus *Dictyotriletes* (including the stratigraphically important species *D. emsiensis* and *D. subgranifer*).

Crassitate trilete spores are also present. The laevigate crassitate spore *Ambitisporites avitus* is relatively abundant. Simple apiculate forms such as *Anapiculatasporites petilus* and *Aneurospora goensis* are less common. *Emphanisporites* is relatively common and diverse (e.g. *E. rotatus*). The next major morphotype of trilete spore are the patinate forms. Laevigate forms (*Archaeozonotriletes chulus*) are relatively common, but ornamented forms are also recorded and include forms belonging to *Chelinospora* (2 species) and *Cymbosporites* (3 species). The stratigraphically important *Clivosispora verrucata* is also present.

Another rare, but conspicuous feature of the assemblages are of the crassitate spores with various modifications to their trilete mark and/or interradial areas (e.g. interradial papillae) and/or distal surfaces. These spores, for example *Synorisporites papillensis*, possibly belong to a closely related group. Such spores are often a common component of Devonian spore assemblages from Brittany (Le Hérissé, 1983) and Spain (Rodriguez, 1983). Zonate spores are present but very rare.

The relatively common species *Camarozonotriletes filatoffii*, *Cymbohilates baqaensis*, *C. comptulus*, *Gneudnaspora divellomedia* var. *minor* and *Scylaspora costulosa* appear at the base of the composite sequence.

7. Biostratigraphy

The oldest spore assemblages from the lower part of the Sha'iba Member are considered to belong to the PoW Oppel Zone of Streel et al. (1987), based on the general characteristics of the assemblages and the presence of characteristic taxa such as *Brochotriletes foveolatus*, *Clivosispora verrucata*, *Dictyotriletes emsiensis*, *D. subgranifer* and *Verrucosisporites polygonalis* (Fig. 2; Appendix A). The presence of *D. subgranifer* may indicate that they belong to the uppermost interval zone (Su Interval Zone) of the PoW Oppel Zone. The PoW Oppel Zone is of Pragian-earliest Emsian age, with the Su Interval Zone straddling the latest Pragian-earliest Emsian. Thus we consider that the oldest spore assemblages from the Sha'iba Member are of late Pragian-earliest Emsian age. No characteristic Emsian taxa (e.g. *Camarozonotriletes sextantii*, *Emphanisporites schultzii*) are recorded.

Higher in the younger parts of Sha'iba Member (Fig. 2; Appendix A) *Gneudnaspora divellomedia* var. *divellomedia* appears and becomes common in the upper part of the composite sequence, whereas the smaller variety, *G. divellomedia* var. *minor* shows an inverse abundance distribution. *Dictyotriletes biornatus* also makes its first appearance at this level.

The simple monolete spore, *Latosporites ovalis*, appears towards the top of the Sha'iba member. It is a relatively uncommon, but persistent, component of the spore assemblages up to the top of the Hammamiyat Member (Fig. 2; Appendix A). This occurrence is particularly interesting as it represents one of the earliest reports of a monolete spore, and hints at the possibility that monolete spores appeared on Gondwana, before their first appearance in Euramerica.

In the Qasr Member, the spore assemblages are essentially homogeneous, but a number of notable species make their inception (Fig. 2; Appendix A). These include the stratigraphically important spores *Emphanisporites schultzii*, and?*Knoxisporites riondae*. Similar spore assemblages are recovered from throughout the Qasr Member (BAQA-1) and lower part of the Subbat Member (BAQA-1 and JNDL-4) (Fig. 2; Appendix A). These spore assemblages are typical of those of Emsian age elsewhere and probably belong to either the AB or lower FD Oppel Zones. *Artemopyra inconspicua* and *A. recticosta* appear within these assemblages and coexist up into the youngest samples. These assemblages are constrained above by the first appearance of *Rhabdosporites minutus* whose inception marks the base of the

FD Oppel Zone (Min Interval Zone) (see below). *Cymbosporites asymmetricus* and *Stellatispora multicostata* appear just below the base of the Min Interval Zone.

An important inception is the first appearance of *Rhabdosporites minutus* towards the top of the Subbat Member in JNDL-4 (Fig. 2; Appendix A). In Euramerica this taxon first appears in the FD Oppel Zone (Min Interval Zone) of late Emsian age. Not far above this, in the lower part of the Hammamiyat Member (also in JNDL-4), the stratigraphically important spore *Camarozonotriletes sextantii* first appears. In the spore biostratigraphic scheme of Richardson and McGregor (1986) *C. sextantii* is a nominal species for the AS Spore Assemblage Biozone of early (but not earliest) to early late Emsian age. These authors note the sporadic occurrence of this taxon: in some sequences it is abundant but in others it is extremely rare. Its inception is variable and its occurrence is intermittent. Thus the presence of *C. sextantii* is consistent with an assignment to the Min Interval Zone and a mid Emsian age. *Cymbohilates heteroverrucosus* makes its inception within the Min Interval Zone and reaches the top of the composite sequence.

The spore assemblages are essentially similar throughout the remainder of the Hammamiyat Member (JNDL-4 and JNDL-3) and the lower part of the Murayr Member (JNDL-3) (Fig. 2; Appendix A). These suites are typical of the late Emsian and probably belong to the upper FD to lower AP Oppel Zones. An interesting feature of this part of the sequence is the sporadic occurrence of palynomorph assemblages dominated by a single sphaeromorph taxon. In these assemblages spores are very rare and acritarchs are much more abundant. The occurrence of these sphaeromorph-dominated assemblages are interesting with respect to the D3B horizon that is considered to be a good marker horizon (e.g. Al-Hajri et al., 1999). Al-Hajri et al. (1999) noted that the D3B palynosubzone is marked by the sudden abundance of a monospecific leiosphaerid (sphaeromorph), and this acme zone is reported as ranging over 5 to 60 ft in cored sections. Our sphaeromorph-dominated assemblages interdigitate with normal spore-dominated assemblages. Furthermore, although some consist predominantly of a single sphaeromorph taxon, others contain numerous different unusual algal palynomorphs (Breuer et al., 2005). If these sphaeromorph-dominated assemblages are related to D3B, the sphaeromorph-dominated horizons represent a peculiar, but recurrent, facies that repeats sharply between more normal spore-dominated facies (Breuer et al., 2005). This series of sudden pulses of sphaeromorph-dominated assemblages (D3B) spans some 400 ft of section and is represented in Fig. 2. Interestingly these conspicuous assemblages occur in both boreholes JNDL-3 and JNDL-4 and the pulses can be correlated between the two cored sections.

In the upper part of the Murayr Member (JNDL-3) and lowermost part of the Jubah Formation (JNDL-1) a number of distinctive species make their last appearance (e.g. *Camarozonotriletes sextantii*, *Clivosispora verrucata*, *Retusotriletes maculatus*, *Verrucosisporites polygonalis*) (Fig. 2; Appendix A) and there is a distinct change in the nature of the spore assemblages. Directly above, *Acinosporites apiculatus* and the zonate form *Grandispora protea* first appear. These indicate the AP Oppel Zone (Pro Interval Zone) of latest Emsian-earliest Eifelian age for the base of the Jubah Formation.

A large gap in recovery follows, with the next spore assemblages being from the middle part of the Jubah Formation (Fig. 2; Appendix A). These spore assemblages are distinctive and very different from those lower in the sequence. They include many zonate-pseudosaccate spores (e.g. *Grandispora douglastownense*, *Samarisporites eximius*, *Zonotriletes armillatus* and *Z. Simplicissimus*) and the stratigraphically important spore, *Geminospora lemurata*. The presence of the latter suggests the AD Oppel Zone (Lem Interval Zone) of early Givetian (Middle Devonian) age. *Camarozonotriletes rugulosus* and *Dibolisporites pilatus* occur within these youngest assemblages.

8. Conclusion

The palynological study of boreholes BAQA-1, BAQA-2, JNDL-1, JNDL-3, and JNDL-4 has allowed the description of one new genus, sixteen new species and one new variety of miospores. This has advanced our knowledge of Lower to Middle Devonian palynofloras of the Arabian Plate. As the stratigraphic palynology presented here is based on species that are common to the well-established Devonian West European zonation of Streel et al. (1987), it documents the ranges of the new endemic species in relation to this well-established zonal scheme. The Euramerican zonation, however, is not ideal for Gondwanan localities, and indeed, not all of the palynozonal subdivisions can be recognized in the BAQA-JNDL succession (see Fig. 2). The near-term goal, upon the study of additional Saudi Arabian successions, is to establish a zonation, incorporating the endemic species, that may be of greater utility for the Arabian Plate and perhaps also other northern and western Gondwanan regions.

Notwithstanding the above shortcomings, the present study has determined a late Pragian to late Emsian age for the Jauf Formation in northern Saudi Arabia with the Pragian/Emsian boundary most likely lying within the upper part of the Sha'iba Member and the Emsian/Eifelian boundary likely within the lower part of the Jubah Formation. Givetian palyno-assemblages (AD-Lem Interval Zone of Streel et al., 1987) are also documented from the Jubah Formation, higher in the succession, but Eifelian assemblages are notably absent. This is believed to be because of a 300 ft, non palyniferous, sandstone interval that separates the productive Emsian and Givetian levels.

Finally, the sphaeromorph-dominated assemblages in the JNDL boreholes can be related to the D3B palynosubzone of Al-Hajri et al. (1999). They represent a series of sudden marine pulses through the Hammamiyat and Murayr members of the Jauf Formation. Palynostratigraphically, they are shown to equate with the FD Min West European zone. The 400 ft stratigraphic span of the D3B interval is much thicker than in eastern Saudi Arabia where it is normally a few tens of feet thick.

Acknowledgements

We are grateful to the management of Saudi Aramco for permission to publish this study. We thank J. Filatoff (Saudi

Aramco) M. Streel (Liège, Belgium) and J.E.A. Marshall (Southampton, UK) for constructive discussions on systematic issues. We acknowledge M. Giraldo-Mezzatesta (Liège) for the preparation of palynological slides. Thanks are also expressed to J.H.G. de Melo (Rio de Janeiro, Brazil) and M. Vecoli (Lille, France) for the review of the manuscript. P. Breuer is supported by a F.R.I.A. grant.

Appendix A. Supplementary data

Supplementary data associated with this article can be found, in the online version, at doi:10.1016/j.revmic.2007.01.009.

References

Al-Hajri, S.A., Filatoff, J., Wender, L.E., Norton, A.K., 1999. Stratigraphy and operational palynology of the Devonian System in Saudi Arabia. GeoArabia 4, 53–68.

Al-Hajri, S.A., Owens, B. (Eds.), 2000. Stratigraphic palynology of the Paleozoic of Saudi Arabia. GeoArabia, Special Publication 1. Gulf PetroLink, Bahrain, pp. 1–231.

Al-Hajri, S.A., Paris, F., 1998. Age and palaeoenvironment of the Sharawra Member (Silurian of northwestern Saudi Arabia. Geobios 31, 3–12.

Allen, K.C., 1965. Lower to Middle Devonian spores of North and Central Vestspitsbergen. Palaeontology 8, 687–748.

Arkhangelskaya, A.D., 1974. Spore-based zonation of the lower part of the Middle Devonian in central and eastern European parts of the USSR. In: Naumova, S.N. (Ed.), Palynology of Proterophyte and Paleophyte. Proceedings of III International Palynological Conference, Nauka, Moscow, pp. 56–59 (in Russian).

Arkhangelskaya, A.D., 1978. Spores from the Lower Devonian of the Lithuanian SSR. Paleontologicheskii Zhurnal 2, 113–120 (in Russian).

Arkhangelskaya, A.D., 1980. Plant spores from some Lower Devonian sections of the western regions of the Russian Plate. In: Byvsheva, T.V. (Ed.), Palynological research in the Proterozoic and Phanerozoic of oil and gas bearing regions of USSR. Trudy Vsesoluznogo Naucho-Issledovatel'skogo Geologoazvedochnogo Neftianogo Instituta (VNIGNI). Moscow, pp. 26–46 (in Russian).

Arkhangelskaya, A.D., 1985. Zonal spore assemblages and stratigraphy of the Lower and Middle Devonian in the Russian Plate. In: Menner, V.V., Byvsheva, T.V. (Eds.), Atlas of spore and pollen from the Phanerozoic petroleum formations in the Russian and Turanian Plates. Trudy Vsesoiuznogo Nauchno-Issledovatel'skogo Geologorazvedochnogo Neftianogo Institute (VNIGNI), Moscow, pp. 5–21 (in Russian).

Beydoun, Z.R., 1991. Arabian Plate hydrocarbon geology and potential - A Plate tectonic approach. American Association of Petroleum Geologists, Studies in Geology 33, 1–77.

Balme, B., 1988. Miospores from Late Devonian (early Frasnian) strata, Carnarvon Basin, Western Australia. Palaeontographica, Abt. B 209, 109–166.

Boucot, A.J., 1984. Old World Realm (Rhenish-Bohemian Region), shallow water, Early Devonian Brachiopods from the Jauf Formation, Saudi Arabia. Journal of Palaeontology 58, 1196–1203.

Boucot, A.J., McClure, H.A., Alvarez, F., Ross, J.P., Taylor, D.W., Struve, W., Savage, N.N., Turner, S., 1989. New Devonian fossils from Saudi Arabia and their biogeographical affinities. Senckenbergiana Lethaea 69, 535–597.

Breuer, P., Al-Ghazi, A., Filatoff, J., Higgs, K.T., Steemans, P., Wellman, C.H., 2005. Stratigraphic palynology of Devonian boreholes from northern Saudi Arabia. In: Steemans, P., Javaux, E. (Eds.), Pre-Cambrian to Palaeozoic Palaeopalynology and Palaeobotany. Carnets de Géologie/Notebooks on Geology, Brest, Memoir 2005/02, Abstract 01.

Buret, M.B., Moreau-Benoît, A., 1986. Données nouvelles apportées par la palynoplanctologie sur la formation des alternances argilo-gréseuses (Silurien supérieur de Libye, bassin de Rhadamès). Comptes Rendus de l'Académie des Sciences de Paris (II/16) 302, 1009–1014.

Burgess, N.D., Richardson, J.B., 1991. Silurian cryptospores and miospores from the type Wenlock area, Shropshire England. Palaeontology 34, 601–628.

Burgess, N.D., Richardson, J.B., 1995. Late Wenlock to early Pridoli cryptospores and miospores from south and southwest Wales, Great Britain. Palaeontographica, Abt. B 236, 1–44.

Chibrikova, E.V., 1959. Spores of the Devonian and older rocks of Bashkiria. Data on palaeontology and stratigraphy of Devonian and older deposits of Bashkiria. Academy of Sciences of USSR, Bashkirian Branch, 1–247 (in Russian).

Clayton, G., Owens, B., Al-Hajri, S.A., Filatoff, J., 2000. Latest Devonian and Early Carboniferous miospore assemblages from Saudi Arabia. In: Al-Hajri, S.A., Owens, B. (Eds.), Stratigraphic palynology of the Paleozoic of Saudi Arabia. GeoArabia Special Publication 1, Bahrain, pp. 146–153.

Cramer, F.H., 1966a. Palynomorphs from the Siluro-Devonian boundary in N.W. Spain. Notas y Comunicaciones del Instituto Geológico y Minero de España 85, 71–82.

Cramer, F.H., 1966b. Hoegispheres and other microfossils *incertae sedis* of the San Pedro Formation (Siluro-Devonian boundary) near Valporquero, Léon, NW Spain. Notas y Comunicaciones del Instituto Geológico y Minero de España 86, 75–94.

Cramer, F.H., 1967. Palynology of Silurian and Devonian rocks in Northwest Spain. Boletín del Instituto Geológico y Minero de España 77, 225–286.

Cramer, F.H., Díez, M.d.C.R., 1975. Earliest Devonian miospores from the province of Leon, Spain. Pollen et Spores 17, 331–344.

de Jersey, N.J., 1966. Devonian spores from the Adavale Basin. Bulletin of the Geological Survey of Queensland, Publication 334. Palaeontology 3, 1–28.

Dufka, P., 1995. Upper Wenlock miospores and cryptospores derived from a Silurian volcanic island in the Prague Basin (Barrandian area, Bohemia). Journal of Micropalaeontology 14, 67–79.

Forey, P.L., Young, V.T., McClure, H.A., 1992. Lower Devonian fishes from Saudi Arabia. Bulletin of the British Museum of Natural History Geology 48, 25–43.

Hemer, D., Nygreen, P., 1967. Devonian palynology of Saudi Arabia. Review of Palaeobotany and Palynology 5, 51–61.

Hoffmeister, W.S., 1959. Lower Silurian plant spores from Libya. Micropaleontology 5, 331–334.

Ibrahim, A.C., 1933. Sporenformen des ägirhorizontes des Ruhrreviers. Dissertation, Technische Hochschule, Berlin.

Ishchenko, A.M., 1952. Atlas of Middle Carboniferous microspores and pollen grains from Donbas. Akademiya Nauk Ukrainskoy SSR, Trudy Instituta Geologischeskikh Nauk, 83 p. (in Russian).

Ishchenko, A.M., 1958. Spore and pollen analysis of the Lower Carboniferous deposits of the Dnieper-Donets Basin. Akademiya Nauk Ukrainskoy SSR, Trudy Instituta Geologischeskikh Nauk, 187 p. (in Russian).

Jansonius, J., Hills, L.V., Hartkopf-Fröder, C., 1998. Genera file of fossil spores – supplement 12. Special Publication, Department of Geology and Geophysics, University of Calgary, Canada.

Jardiné, S., Yapaudjian, L., 1968. Lithostratigraphie et palynologie du Dévonien-Gothlandien gréseux du Bassin de Polignac (Sahara). Revue de l'Institut Français du Pétrole 23, 439–469.

Kemp, E.M., 1972. Lower Devonian palynomorphs from the Horlick Formation, Ohio range, Antarctica. Palaeontographica, Abt. B 139, 105–124.

Lanninger, E.P., 1968. Sporen-Gesellschaften aus dem Ems der SW-Eifel (Rheinisches Schiefergebirge). Palaeontographica, Abt. B 122, 95–170.

Le Hérissé, A., 1983. Les spores du Dévonien inférieur du Synclinorium de Laval (Massif Armoricain). Palaeontographica, Abt. B 188, 1–81.

Lele, K.M., Streel, M., 1969. Middle Devonian (Givetian) plant microfossils from Goé (Belgium). Annales de la Société Géologique de Belgique 92, 89–121.

Loboziak, S., 2000. Middle to Late Devonian miospore biostratigraphy of Saudi Arabia. In: Al-Hajri, S.A., Owens, B. (Eds.), Stratigraphic palynology of the Paleozoic of Saudi Arabia. GeoArabia Special Publication 1, Bahrain, pp. 134–145.

Loboziak, S., Streel, M., 1989. Middle-Upper Devonian miospores from the Ghadamis Basin (Tunisia-Libya): Systematics and stratigraphy. Review of Palaeobotany and Palynology 58, 173–196.

Loboziak, S., Streel, M., 1995. Late Lower and Middle Devonian miospores from Saudi Arabia. In: Owens, B., Al-Tayyar, H., Van der Eem, J.G. (Eds.), Palaeozoic palyno stratigraphy of the Kingdom of Saudi Arabia. Review of Palaeobotany and Palynology 89, Amsterdam, pp. 105–113.

Luber, A.A., Waltz, I.E., 1938. Klassifikatsiya i stratigraphicheskoe znachenie spor nekotorich kammenoughol'nich mestorojdenii SSSR. Trudy TSNIGRI, Moscow 105, 1–45 (in Russian).

Magloire, L., 1968. Étude stratigraphique par la palynologie des dépôts argilo-gréseux du Silurien et du Dévonien inférieur dans la région du Grand Erg Occidental (Sahara algérien). In: International Symposium on the Devonian System Calgary, 2, 473–495.

McGregor, D.C., 1960. Devonian spores from Melville Island Canadian Artic Archipelago. Palaeontology 3, 26–44.

McGregor, D.C., 1961. Spores with proximal radial pattern from the Devonian of Canada. Geological Survey of Canada Bulletin 76, 1–11.

McGregor, D.C., 1973. Lower and Middle Devonian spores of Eastern Gaspé, Canada. Palaeontographica, Abt. B 142, 1–77.

McGregor, D.C., 1974. Early Devonian spores from central Ellesmere Island Canadian Artic. Canadian Journal of Earth Sciences 11, 70–78.

McGregor, D.C., 1984. Late Silurian and Devonian spores from Bolivia. Academia Nacional de Ciencias 69, 1–57.

McGregor, D.C., Camfield, M., 1976. Upper Silurian? to Middle Devonian spores of the Moose River Basin, Ontario. Geological Survey of Canada, Bulletin 263, 1–63.

McGregor, D.C., Camfield, M., 1982. Middle Devonian miospore from the Cape de Bray, Weatherall, and Hecla Bay Formations of northeastern Melville Island, Canadian Artic. Geological Survey of Canada, Bulletin 348, 1–105.

McGregor, D.C., Narbonne, G.M., 1978. Upper Silurian trilete spores and other microfossils from the Read Bay Formation, Cornwallis Island Canadian Arctic. Canadian Journal of Earth Sciences 15, 1292–1303.

Meissner Jr., C.R., Dini, S.M., Farasani, A.M., Riddler, G.P., van Eck, M., Aspinall, N.C., 1988. Preliminary geological map of the Al Jawf quadrangle, sheet 29D, Kingdom of Saudi Arabia. In: Open-file report, USGS-OF-09-1, Ministry of Petroleum and Minerals, Deputy Ministry for Mineral Resources, Jeddah.

Moreau-Benoît, A., 1965. Premiers résultats d'une étude palynologique du Dévonien de la carrière des Fours à Chaux d'Angers (Maine-et-Loire). Revue de Micropaléontologie 9, 219–240.

Moreau-Benoît, A., 1976. Les spores et débris végétaux, Les Schistes et Calcaires éodévoniens de Saint-Cénéré (Massif armoricainFrance). Mémoires de la Société géologiques et minéralogique de Bretagne 19, 27–58.

Naumova, S.N., 1953. Spore-pollen assemblages of the Upper Devonian of the Russian Platform and their stratigraphic significance. Transactions of Institute of Geological Sciences of the USSR 143,, 204 p. (in Russian).

Owens, B., 1971. Miospores from the Middle and Early Upper Devonian rocks of the Western Queen Elizabeth Island, Arctic Archipelago. Geological Survey of Canada 70, 1–157.

Playford, G., 1983. The Devonian miospore genus *Geminospora* Balme, 1962: reappraisal based upon topotypic *G. lemurata* (type species). Memoir of the Association of Australasian Palaeontologists 1, 311–325.

Potonié, R., Kremp, G., 1954. Die Gattungen der paläozoischen *Sporae dispersae* und ihre Stratigraphie. Geologisches Jahrbuch 69, 111–194.

Powers, R.W., 1968. Asie: Arabie Saoudite. Lexique Stratigraphique International. Éditions du CNRS, Paris, 177 p.

Powers, R.W., Ramirez, L.F., Redmond, C.D., Elberg Jr., E.L., 1966. Sedimentary Geology of Saudi Arabia. In: Geology of the Arabian Peninsula. United States Geological Survey, Professional Paper, 560D, Washington, pp. 1–147.

Richardson, J.B., 1965. Middle Old Red Sandstone spore assemblages from the Orcadian basin north-east Scotland. Palaeontology 7, 559–605.

Richardson, J.B., 1996. Taxonomy and classification of some new Early Devonian cryptospores from England. In: Cleal, C.J. (Ed.), Studies on early land plant spores from Britain. Special Papers in Palaeontology 55, Oxford, pp. 7–40.

Richardson, J.B., Lister, T.R., 1969. Upper Silurian and Lower Devonian spore assemblages from the Welsh Borderland and South Wales. Palaeontology 12, 201–252.

Richardson, J.B., McGregor, D.C., 1986. Silurian and Devonian spore zones of the Old Red Sandstone continent and adjacent regions. Geological Survey of Canada, Bulletin 364, 1–79.

Richardson, J.B., Streel, M., Hassan, A., Steemans, P., 1982. A new spore assemblage to correlate between the Breconian (British Isles) and the Gedinnian (Belgium). Annales de la Société Géologique de Belgique 105, 135–143.

Richardson, J.B., Rasul, S.M., 1978. Palynomorphs in Lower Devonian sediments from the Apley Barn borehole, Southern England. Pollen et Spores 20, 423–462.

Richardson, J.B., Rodriguez, R.M., Sutherland, S.J.E., 2001. Palynological zonation of Mid- Palaeozoic sequences from the Cantabrian Mountains, NW Spain: implications for inter-regional and interfacies correlation of the Ludford/Prídolí and Silurian/Devonian boundaries, and plant dispersal patterns. Bulletin Natural History Museum London (Geology) 57, 115–162.

Riegel, W., 1968. Die Mitteldevon-Flora von Lindlar (Rheinland). 2. Sporae dispersae. Palaeontographica, Abt. B 123, 76–96.

Riegel, W., 1973. Sporenformen aus den Heisdorf-Lauch- und Nohn-Schichten (Emsium und Eifelium) der Eifel, Rheinland. Palaeontographica. Abt. B 142, 78–104.

Rodriguez, R.M., 1983. Palinología de las formaciones del Silúrico superior - Devonico inferior de la Cordillera Cantabrica. Servício de Publicaciones, Universidad de León, León, 231 p.

Rubinstein, C., Steemans, P., 2002. Miospore assemblages from the Silurian-Devonian boundary, in borehole A1-61, Ghadamis Basin, Libya. In: Steemans, P., Servais, T., Streel, M. (Eds.), Paleozoïc Palynology: a special issue in honour of Dr. Stanislas Loboziak. Review of Palaeobotany and Palynology 118, Amsterdam, pp. 397–421.

Schopf, J.M., Wilson, L.R., Bentall, R., 1944. An annotated synopsis of Paleozoic fossil spores and the definition of generic groups. Illinois State Geological Survey, Report of Investigations 91, 1–66.

Sharland, P.R., Archer, R., Casey, D.M., Davies, R.B., Hall, S.H., Heward, A.P., Horbury, A.D., Simmons, M.D., 2001. Arabian Plate sequence stratigraphy. GeoArabia Special Publication 2, Gulf PetroLink, Bahrain, pp. 1–371.

Steemans, P., 1989. Palynostratigraphie de l'Eodévonien dans l'ouest de l'Europe. Mémoires Explicatifs pour les Cartes Géologiques et Minéralogiques de la Belgique 27. Service Géologique de Belgique, Bruxelles, 453 p.

Steemans, P., 1995. Silurian and Lower Emsian spores in Saudi Arabia. Review of Palaeobotany and Palynology 89, 91–104.

Steemans, P., Le Hérissé, A., Bozdogan, N., 1996. Ordovician and Silurian cryptospores and miospores from Southeastern Turkey. Review of Palaeobotany and Palynology 93, 35–76.

Steemans, P., Higgs, K.T., Wellman, C.H., 2000. Cryptospores and trilete spores from the LlandoveryHaweiyah 151 from Saudi Arabia. In: Al-Hajri, S., Owens, B. (Eds.), Stratigraphic Palynology of the Palaeozoic of Saudi Arabia. GeoArabia Special Publication 1, Bahrain, pp. 92–115.

Steineke, M., Bramkamp, R.A., Sander, N.J., 1958. Stratigraphic relations of Arabian oil. In: Weeks, L.G. (Ed.), Habitat of oil. American Association of Petroleum Geologists, Symposium Tulsa, pp. 1294–1329.

Streel, M., 1964. Une association de spores du Givétien inférieur de la Vesdre à Goé (Belgique). Annales de la Société Géologique de Belgique 87, 1–30.

Streel, M., 1967. Associations de spores du Dévonien inférieur belge et leur signification stratigraphique. Annales de la Société Géologique de Belgique 90, 11–53.

Streel, M., Higgs, K.T., Loboziak, S., Riegel, W., Steemans, P., 1987. Spore stratigraphy and correlation with faunas and floras in the type marine Devonian of the Ardenne-Rhenish region. Review of Palaeobotany and Palynology 50, 211–219.

Strother, P.K., Traverse, A., 1979. Plant microfossils from the Llandoverian and Wenlockian rocks of Pennsylvania. Palynology 3, 1–21.

Stump, T.E., Al-Hajri, S.A., Van der Eem, J.G., 1995. Geology and biostratigraphy of the Late Precambrian through Palaeozoic sediments of Saudi Arabia. In: Owens, B., Al-Tayyar, H., Van der Eem, J.G. (Eds.), Palaeozoic palynostratigraphy of the Kingdom of Saudi Arabia. Review of Palaeobotany and Palynology 89, Amsterdam, pp. 5–17.

Tiwari, R.S., Schaarschmidt, F., 1975. Palynological studies in the Lower and Middle Devonian of the Prüm SynclineEifel (Germany). Abhandlungen der Seckenbergischen Naturforschenden Gesellschaft 534, 1–129.

Turnau, E., 1986. Lower to Middle Devonian spores from the vicinity of Pionki (Central Poland). Review of Palaeobotany and Palynology 46, 311–354.

Turnau, E., Milaczewski, L., Wood, G.D., 2005. Spore stratigraphy of Lower Devonian and Eifelian (?), alluvial and marginal marine deposits of the Radom-Lublin area (central Poland). Annales Societatis Geologorum Poloniae 75, 121–137.

Wellman, C.H., 1993. A Lower Devonian sporomorph assemblage from the Midland Valley of Scotland. Transactions of the Royal Society of Edinburgh: Earth Sciences 84, 117–136.

Wellman, C.H., 2007. Spore assemblages from the Lower Devonian 'Lower Old Red Sandstone' deposits of the Rhynie Outlier, Scotland. Transactions of the Royal Society of Edinburgh: Earth Sciences 97, 167–211.

Wellman, C.H., Richardson, J.B., 1996. Sporomorph assemblages from the 'Lower Old Red Sandstone' of Lorne Scotland. In: Cleal, C.J. (Ed.), Studies on early land plant spores from Britain. Special Papers in Palaeontology 55, Oxford, pp. 41–101.